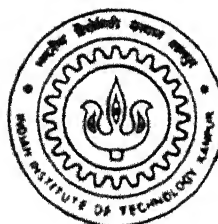


2-D PHASE RETRIEVAL : A WAVELET APPROACH

by

Maj Subroto Ganguly



TH
EE/1999/M
5155-P

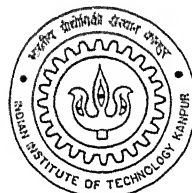
DEPARTMENT OF ELECTRICAL ENGINEERING
INDIAN INSTITUTE OF TECHNOLOGY KANPUR

April, 1999

2-D PHASE RETRIEVAL : A WAVELET APPROACH

A Thesis Submitted
in Partial Fulfillment of the Requirements
for the Degree of
Master of Technology

by
Maj Subroto Ganguly



to the
DEPARTMENT OF ELECTRICAL ENGINEERING
INDIAN INSTITUTE OF TECHNOLOGY, KANPUR
April, 1999

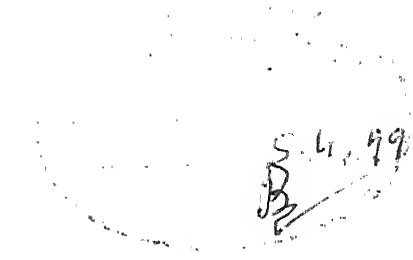
4 Aug 1991

2

2

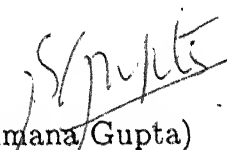
128769





Certificate

It is certified that the work contained in this thesis entitled 2-D PHASE RETRIEVAL: A WAVELET APPROACH, by Maj S Ganguly, has been carried out under my supervision and that this work has not been submitted elsewhere for a degree.



(Dr. Sumana Gupta)

Associate Professor

Dept. of Electrical Engineering

Indian Institute of Technology

Kanpur

5th April, 1999

To
Corps Of EME

Acknowledgements

I would like to express my sincere gratitude to Dr. Sumana Gupta for her invaluable guidance and constant encouragement in completing my thesis work. She has been very helpful throughout the duration of the thesis.

Also I would love to mention the names of Ashok, Arindam, Sandhitsu, Joyshree, Shafiullah, Mrs Bhoosan Lal, Ajay and Balkishan , who have all helped me at some stage or other.

I wish to acknowledge the support, my wife Nupur and daughter Mani gave me all along and the blessings our parents always have for us.

Abstract

Phase retrieval from the measurements of the Fourier modulus is an important and difficult problem. Among all the approaches developed to solve the problem so far, the iterative transform algorithms are currently the most efficient. However these algorithms suffer from major drawbacks that limit their practical applications. In this thesis the direct method i.e., the iterative transform method as well as wavelet based method of phase retrieval is being presented with the aim to discuss the means to improve the performance of the algorithms leading to better phase retrieval quality.

It is being established that wavelet based method of phase retrieval increases the computational efficiency by over 60% in many cases while at the same time obtaining reduction in residual reconstruction error (upto 20%) as compared to the direct method. Further the quality criterion of wavelets chosen for subspace signal decomposition has an influence over the phase retrieval error and quality to a varying degree is being established.

Contents

1	Introduction	1
1.1	Phase Retrieval From Partial Information	3
1.1.1	Error-Reduction Algorithm	5
1.1.2	Steepest Descent Method	6
1.1.3	Other Gradient Search Methods	7
1.1.4	Input-Output Algorithms	9
1.1.5	Additional Methods	11
1.2	OVERVIEW	12
2	The Multiresolution Analysis	13
2.1	Wavelets : A Review	14
2.1.1	Wavelets : Construction	14

2.1.2	Wavelet Decomposition	15
2.1.3	Two Dimensional Wavelet Decomposition	17
2.2	Multiresolution Analysis: The basic idea	18
2.3	Quality Criterion For Wavelets Used In Image Processing	23
3	Phase Retrieval	32
3.1	Introduction	32
3.2	Fourier synthesis from partial information: Importance of phase	33
3.3	Phase retrieval problem : The uniqueness question	41
3.3.1	Uniqueness :Revisited	42
3.4	Direct Approach:The Fienup Algorithm	43
3.4.1	Convergence for the algorithm	45
3.4.2	Additional aspects of the Fienup algorithm	46
3.5	Wavelet method :The Multiresolution approach	49
3.5.1	The algorithm	50
3.6	Ambiguity Correction	53
3.7	Fourier coefficient truncation	54

4 Reconstruction experiments and results	56
4.1 Fienup Reconstructions	56
4.2 Multiresolution wavelet based reconstructions	58
4.2.1 Characteristics of the wavelets used	59
4.2.2 Algorithm	62
4.3 Ambiguity correction results	66
4.4 Fourier coefficient truncation results	68
4.5 Discussions	72
5 Conclusions And Scope For Future Work	79
5.1 Scope for future work	80
Bibliography	81

List of Figures

1.1	Block diagram- Gradient Search method	9
1.2	Block diagram: Input Output concept	10
2.1	Illustration of a Wavelet and the corresponding Scaling Function. Also illustrated is the Fourier modulus of the scaling function. Wavelet is a band pass filter.	27
2.2	Illustration of an orthogonal and a biorthogonal Wavelet and their corresponding Scaling Functions	28
2.3	Wavelet Decomposition	29
2.4	Wavelet Reconstruction	29
2.5	2-D Wavelet Decomposition	30
2.6	2-D Wavelet Reconstruction	30
2.7	Decomposition Of A Two Dimensional Signal Down To Level 4	31
2.8	Illustration of wavelet decomposition of an Image down to two levels .	31

3.1	Phase only synthesis (a) original image and (b) the image synthesised using complete phase information and constant magnitude function	34
3.2	Magnitude only synthesis (a) original image and (b) the image synthesised using complete magnitude information and 1-bit phase function	36
3.3	Magnitude only synthesis (a) original image and (b) the image synthesised using complete magnitude information and 1-bit phase function	37
3.4	Magnitude only synthesis (a) original image and (b) the image synthesised using complete magnitude information and zero phase function	39
3.5	Magnitude only synthesis (a) original image and (b) the image synthesised using complete magnitude information of cameraman image and phase function from bird image	40
3.6	Magnitude only synthesis shows magnitude information of bird image and phase function from cameraman image	41
4.1	Phase retrieval by Fienup algorithm. Clockwise two images (1) original <i>Figure 10</i> . (2) initial input guess, (3) to (6) are reconstructions at increasing iterations.	58
4.2	Phase retrieval by Fienup algorithm.(a) original <i>Saturn</i> (b) initial guess and (c) Final reconstructed image after 11 cycles	59
4.3	Reconstruction error for <i>Saturn</i> using Fienup algorithm for 11 cycles	60
4.4	Reconstruction error for <i>Figure 10</i> using Fienup algorithm for 11 cycles	61

4.5	Filter coefficients and frequency responses of selected Daubachies wavelets. Clockwise from top left (a) db1 ; High(*) and low pass(o) decomposition wavelets (b) db5 (c) Frequency response of the wavelets; o shows db1, * shows db5 and + shows db9 low pass decomposition wavelet frequency response. (d) db9.	62
4.6	Filter coefficients and frequency responses of selected B-Spline Biorthogonal wavelets. Clockwise from top left (a) Bior1.1 ; High(*) and low pass(o) decomposition wavelets. (b) bior4.4 (c) Frequency response of the wavelets, o shows bior1.1, * shows bior4.4 and + shows bior6.8 low pass decomposition wavelet frequency response.(d) bior6.8.	63
4.7	Comparative Fourier moduli of db1 (indicated on plot by o), db5(*) and db9(+). All decomposition low pass characteristics.	64
4.8	Comparative Fourier moduli of bior4.4(indicated on plot by o) and bior6.8(*). All decomposition low pass characteristics.	64
4.9	Phase retrieval by Wavelet algorithm using db5 wavelet.Clockwise from left top (a) original <i>Saturn</i> (b) initial guess and (1) Final reconstructed image at resolution 32×32 (2) reconstruction at level 64×64 resolution (3) to (7) reconstructions at increasing level of iterations for full resolution	66
4.10	Phase retrieval by Wavelet algorithm using db1 wavelet. Clockwise from left top (a) original <i>Saturn</i> (b) Final reconstructed image at resolution 32×32 (c) reconstruction at level 64×64 resolution (d) reconstruction after 11 cycles at full resolution	67

4.11 Phase retrieval by Wavelet algorithm using B-Spline Biorthogonal wavelet Bior4.4. Clockwise from left top (a) original <i>Figure 10</i> (b) Final reconstructed image at resolution 32×32 (c) reconstruction at level 64×64 resolution (d) reconstruction after 11 cycles at full resolution	68
4.12 Phase retrieval by Wavelet algorithm using db1 wavelet.(a) original <i>Claire</i> (b) Final reconstructed image at resolution 256×256 after 11 cycles at full resolution. Note that inspite of increasing the Fourier resolution, only outlines of the subject could be retrieved indicating the limitations of multiresolution phase retrieval for detailed image reconstruction with only Fourier modulus.	69
4.13 Reconstruction errors for <i>Saturn</i> using wavelet based approach for first seven cycles of iterations.(a) Using Bior6.8 wavelet (b) db1 (c) db5 (d) db9 and finally (e) Bior4.4. Convergence pattern remains same upto 11 cycles.	70
4.14 Reconstruction errors for <i>Figure 10</i> using wavelet based approach for first seven cycles of iterations. (a) Using Bior6.8 wavelet (b) db1 (c) db5 (d) db9 and finally (e) Bior4.4. Convergence pattern remains uncertain upto 7 cycles wherein the mask was increased. Note that the input to the full resolution algorithm by db1 wavelet is lesser than all others.	71
4.15 Reconstruction errors for <i>Figure 10</i> using wavelet based approach for 8 – 11 cycles of iterations.(a) Using Bior6.8 wavelet (b) db1 (c) db5 (d) db9 and finally (e) Bior4.4.	72

4.16 Ambiguity Corrections (a) Phase retrieved image obtained by using db5 wavelet. Note the translation and reversal ambiguities. (b) Translation ambiguity corrected image (c) Reversal ambiguity correction superimposed to get the final phase retrieved image.	73
4.17 Reconstruction of images with truncated Fourier coefficients. (a) Phase retrieved images with db1 wavelet (b) Images obtained by preserving 50% of Fourier coefficients. All others are set to 0. (c) Same with 12% of the coefficients preserved.	78

List of Tables

4.1	Reconstruction error comparisons <wavelet Vs Fienup> on image <i>Saturn</i>	65
4.2	Reconstruction error comparisons < wavelet Vs Fienup> on <i>Figure 10</i> 73	
4.3	Reconstruction with truncated Fourier Coefficients	74

Chapter 1

Introduction

Image reconstruction given partial information about its spectral contents remains an important and difficult problem. Although there is a one to one correspondence between a signal and its Fourier transform there are many applications [2] in which some of the Fourier domain information is either degraded or missing. The examples include Imaging through a turbulent atmosphere, X-ray Crystallography, Seismological and Ocean Acoustics applications and Astronomical Imaging/Applications. In order to restore the signal, therefore, it is desirable to recover the missing spectral information. An important area of investigation in such applications is to recover the complete loss of either Phase or Magnitude information. Also in the absence of any underlying signal model or constraints and also any *a priori* knowledge of signal, the loss of either Phase or Magnitude information of a complex function is considered irreversible.

However although phase or magnitude alone is not sufficient, in general, to uniquely specify a sequence, yet under a variety of constraints an approximate signal may be synthesised in such a way that the information in original signal is fairly

represented in the synthesised signal even though the synthesised signal may not be an accurate representation on a point to point basis. The ability to reconstruct a signal from only phase or magnitude information alone would be useful in all such applications. To illustrate, for example in the case of problems referred to as *Blind Deconvolution* , a desired signal is to be recovered from an observation which is the convolution of the desired signal with some unknown signal. Since little is usually known about either the desired signal or the distorting signal, deconvolution of the two signals is generally a difficult problem. However, in the special case in which the distorting signal is known to have a Zero phase characteristics, the phase of the desired signal is undistorted. Such a situation is at least approximately known to occur in long term exposure to atmospheric turbulence. In this case the phase of the observed signal is approximately the same as the phase of the desired signal and, therefore, it is of interest to consider signal reconstruction from phase information alone.

In this thesis the reconstruction of a *2-Dimensional* (2-D) sequence from its Fourier Transform magnitude has been investigated in the framework of Uniresolution (Single grid) and Multiresolution Wavelet based approaches. It is supposed that the Fourier Modulus $|\chi_0(\mu, \nu)|$ of a real and non negative object $x_0(m, n)$ is given. The reconstruction problem is hence to find a real and nonnegative unique solution $x(m, n)$ so that $|X(\mu, \nu)| = |\chi_0(\mu, \nu)|$. Since

$$DFT[x(m, n)] = \chi(\mu, \nu) = |\chi(\mu, \nu)| e^{j\phi(\mu, \nu)}$$

with $|X(\mu, \nu)| = |\chi_0(\mu, \nu)|$, the reconstruction of the object is equivalent to reconstruction of the Fourier phase $\phi(\mu, \nu)$ from the magnitude (and hence the name *Phase Retrieval*).

Many algorithms have been developed in the past to solve this problem[2,4]

and currently the most preferred algorithms are the Iterative Transform Algorithm and its variants. However these algorithms suffer from three major disadvantages.

(a) Stagnation due to attractions to some local minima which causes the estimate to be trapped and subsequent non convergence. (b) Intensive computations due to the repeated requirement of 2-D DFTs at each cycle /iterations. (c) Lack of good criterion for choosing the initial guess to give the algorithm a better and unbiased chance of convergence.

The platform for the current investigations are hence the Iterative Transform Algorithm (hereinafter referred to as Fienup algorithm), its reconstruction properties, error convergence and quality of reconstruction on different classes of images. The variant of Fienup Algorithm i.e the Hybrid Input-Output has also been clubbed into the basic Fienup Algorithm for escaping possible local stagnation basins. The multiresolution analysis of the same images have been carried out and the parameters examined by using different wavelet bases.

1.1 Phase Retrieval From Partial Information

In electron microscopy, wave front sensing, astronomy, crystallography, and in other fields one often wishes to recover phase, although only intensity measurements are made. One is usually interested in determining an object, $f(x)$, which is related to its Fourier transform, $F(u)$, by

$$\begin{aligned} F(u) &= |F(u)| \exp[i\psi(u)] = \mathcal{F}[f(x)] \\ &= \int_{-\infty}^{+\infty} f(x) \exp(-i2\pi u \cdot x) dx \end{aligned}$$

where x is an M -dimensional spatial coordinate, and u is an M -dimensional

spatial frequency coordinate. For the majority of imaging problems however $M=2$. In practice for sampled data and assuming square arrays, $u = (u_1, u_2)$ and $x = (x_1, x_2)$, where u_1, u_2, x_1 , and $x_2 = 0, 1, 2, \dots, N - 1$. Then one uses the DFT

$$F(u) = \sum_{x=0}^{N-1} f(x) \exp(-i2\pi u \cdot x/N)$$

and its inverse

$$f(x) = N^{-2} \sum_{u=0}^{N-1} F(u) \exp(i2\pi u \cdot x/N)$$

which are computed using the FFT method.

For the problem of recovering phase from two intensity measurements, as in electron microscopy and in wave front sensing,

$$f(x) = |f(x)| \exp[i\eta(x)]$$

is complex valued, and one wishes to recover $\psi(u)$ or equivalently recover $\eta(x)$ from measurement of both $|F(u)|$ and $|f(x)|$. For the problem of recovering phase from a single intensity measurement, as in image recovery from interferometry data in astronomy and from structure factors in crystallography, one wishes to recover $\psi(u)$ or equivalently recover $f(x)$ given a measurement of $|F(u)|$ and the constraint that $f(x)$ be real and nonnegative,

$$f(x) \geq 0$$

A particularly successful approach to solving these problems is the use of Fienup and related algorithms. These algorithms involve iterative Fourier transformation back and forth between the object and Fourier domains and application of the measured data and known constraints in each domain.

In what follows a generalised Fienup algorithm, alternative Gradient search methods and iterative Fourier transform algorithms are described for the case of single intensity measurements.

1.1.1 Error-Reduction Algorithm

The predecessor of Fienup Algorithm, the Gerchberg-Saxton algorithm was originally invented in connection with the problem of reconstructing phase from two intensity measurements(given intensity constraints in each of the two domains). The algorithm consists of the following four steps : (1) Fourier transform an estimate of the object; (2) Replace the modulus of the resulting computed Fourier transform with the measured modulus to form an estimate of the Fourier transform; (3) Inverse Fourier transform the estimate of the Fourier transform; and (4) Replace the modulus of the resulting computed image with the measured object modulus to form a new estimate of the object. In equations this is ,for the k th iteration,

$$\begin{aligned} G_k(u) &= |G_k(u)| \exp[i\phi_k(u)] = \mathcal{F}[g_k(x)] \\ G'_k(u) &= |F(u)| \exp[i\phi_k(u)] \\ g'_k(x) &= |g'_k(x)| \exp[i\theta'_k(x)] = \mathcal{F}^{-1}[G'_k(u)] \\ g_{k+1}(x) &= |f(x)| \exp[i\theta_{k+1}(x)] = |f(x)| \exp[i\theta'_k(x)] \end{aligned}$$

where g_k, θ_k, G'_k , and ϕ_k are estimates of f, η, F , and ψ respectively. As enumerated above the Gerchberg Saxton algorithm can be used for any problem in which partial constraints are known in each of the two domains. One only transforms back and forth between the two domains, satisfying the constraints in one before returning to the other.

For the most general problem the error reduction algorithm consists of the following four steps: (1) Fourier transform $g_k(x)$, an estimate of $f(x)$; (2) Make the minimum changes in $G_k(u)$, the resulting computed Fourier transform ,which allow it to satisfy the Fourier-domain constraints to form $G'_k(u)$, an estimate of $f(u)$; (3) Inverse Fourier transform $G'_k(u)$; and (4) Make the minimum changes in $g'_k(x)$, the resulting computed image, which allow it to satisfy the object domain constraints

to form $g_{k+1}(x)$, a new estimate of the object. In particular for the problem of the single intensity measurement(as in astronomy) the first three steps are identical to the first three steps of the Gerchberg Saxton algorithm, and the fourth step is given by

$$g_{k+1}(x) = \begin{cases} g'_k(x) & x \notin \gamma \\ 0, & x \in \gamma \end{cases}$$

where γ is the set of points at which $g'_k(x)$ violates the object domain constraints, i.e., wherever $g'_k(x)$ is negative or where it exceeds the known diameter of the object. The diameter estimate can be taken since it will be roughly half the diameter of the autocorrelation function, which is the inverse Fourier transform of the squared Fourier modulus. The iterations continue until the computed Fourier transform satisfies the Fourier-domain constraints or the computed image satisfies the object domain constraints ; then one has found a solution, a Fourier transform pair that satisfies all the constraints in both domains.

1.1.2 Steepest Descent Method

An alternative approach to solving the phase retrieval problem is to employ one of the gradient search methods. The Steepest Descent method is closely related to the Error Reduction algorithm for the problem of reconstructing phase from single intensity measurement.

An example of how this gradient search method will be used for our problem follows. One can define say $B = E_F^2$, the squared error in Fourier domain given by the following equations as the error metric which one seeks to minimise by varying a set of parameters.

$$B_k = E_{Fk}^2 = N^{-2} \sum_u [|G_k(u)| - |F(u)|]^2$$

$$B = N^{-2} \sum_u |G(u) - G'(u)|^2$$

Here the N^2 values of $g(x)$, the estimate of $f(x)$ are treated as N^2 independent parameters. Starting at a given point, $g_k(x)$, in the N^2 - dimensional parameter space, one would reduce the error by computing the partial derivatives of B with respect to each of the points $g(x)$ (N^2 partial derivatives) forming the gradient and then move from $g_k(x)$ in a direction opposite to that of the gradient to a new point $g_k''(x)$. One would then form a new estimate, $g_{k+1}(x)$, from $g_k''(x)$ by forcing the object domain constraints to be satisfied. This would be done iteratively with suitable step sizes until a minimum is found (problems of minima whether Global or Local needs to be taken care of still). The above means that one minimises the error, B , as a function of the N^2 parameters, $g(x)$, subject to the object domain constraints.

Ordinarily the computation of the N^2 partial derivatives would be very lengthy task since each evaluation of B involves an $N \times N$ DFT. However, for the problem of single intensity measurement considered here the computations can be greatly reduced by existing methods [6]. In effect the computation of $g(x)$, becomes more or less identical to the first three steps of the Error Reduction algorithm.

The steepest descent method has been known to take more computations and time for convergence than the Error Reduction algorithm. #

1.1.3 Other Gradient Search Methods

As stated in previous section for the phase problem of a single intensity measurement the Steepest Descent method is equivalent to the Error Reduction algorithm. Also

in practice the Error Reduction algorithm converges very slowly for the problem of single intensity measurement. Slower convergence of the Steepest Descent method has been observed for other applications as well [6]. Therefore the need of other gradient search methods. The Steepest descent method moves from the point $g_k(x)$ in parameter space to the point

$$g_k''(x) = g_k(x) - h_k \partial_g B_k \quad (1.1)$$

where h_k , the step size, is a positive constant, and the gradient is given by

$$\partial_g B = 2[g(x) - g'(x)]$$

where $\partial_g B$ is the partial derivative of error B with respect to a value at a given point, $g(x)$. For many applications one would search along the direction of $-\partial_g B_k$, evaluating B repeatedly until the value of h_k that minimises B is found; then from that point one would recompute the gradient and go off in a new direction.

A useful block diagram representation of the family of gradient search methods is shown as fig. 1.1.

A gradient search method superior to the steepest Descent method is the conjugate-gradient method. For this method Eqn.1.1 is replaced by

$$g_k''(x) = g_k(x) + h_k D_k(x)$$

where the direction $D_k(x)$ is given by

$$D_k(x) = g_k'(x) - g_k(x) + (B_k/B_{k-1})D_{k-1}(x)$$

where one would start the first iteration with $D_1(x) = g_1'(x) - g_1(x)$. After employing the above eqns., one would employ the spatial domain support constraints to form the new estimate as indicated in fig.

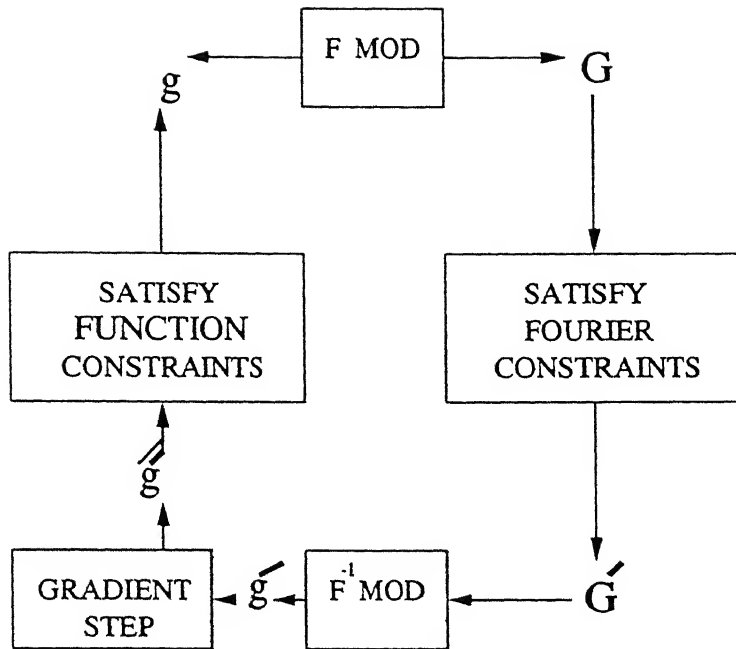


Figure 1.1: Block diagram- Gradient Search method

A further method for this problem apart from the numerous other variations of the gradient search methods is the Newton-Raphson or the Damped Least Squares method. However each iteration of this method involves inversion of an $N^2 \times N^2$ matrix while in the same time a large number of iterations of the gradient search method can be performed and therefore the Newton Raphson method although more sophisticated yet is not preferred.

1.1.4 Input-Output Algorithms

A solution to the problem of the slow convergence of the error-reduction algorithm has been the Input-Output algorithm, which has proved to converge faster for both the problem of two intensity as well as one intensity measurement. The input-output algorithm differs from error-reduction algorithm only in the object domain operation.

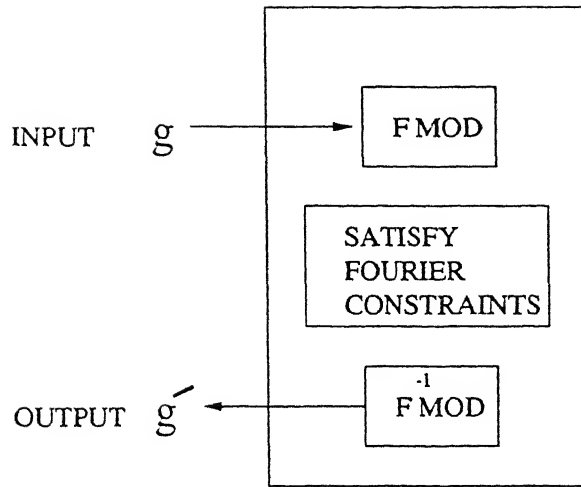


Figure 1.2: Block diagram: Input Output concept

The first three operations -Fourier transforming $g(x)$, satisfying the Fourier-domain constraints, and inverse Fourier transforming the results- are the same for both algorithms. If grouped together as indicated in Fig.1.2 ,these three operations can be thought of as a nonlinear system having an input $g(x)$ and an output $g'(x)$. The notable property of this system is that its output is always an image having a Fourier transform that satisfies the Fourier domain constraints. Therefore if the output also satisfies the object domain constraints than that is the solution to the problem.

It is evident that small change of the input results in a change of the output in the same general direction as the change of the input. More precisely, for a small change of the input the value of the corresponding change of the output is a constant α times the change of the input. Due to additional non linearity the corresponding prediction of output cannot be done exactly yet by appropriate change in the input, the output can be pushed in the general direction desired. If a change $\Delta g(x)$ is desired in the output, a logical choice of the change of the input to achieve that change of the output would be $\beta \Delta g(x)$, where β is a constant(ideally equal to α^{-1}).

For the case of Input-Output algorithm hence the next input is taken as (one of the many other choices)

$$\begin{aligned} g_{k+1}(x) &= g'_k(x) + \beta \Delta g_k(x) \\ &= \begin{cases} g_k(x), & x \notin \gamma \\ g'_k(x) - \beta g'_k(x), & x \in \gamma \end{cases} \end{aligned}$$

The use of above Eqn. is referred to as the Input-Output algorithm. If $\beta = 1$ the same becomes the Error-reduction algorithm.

Still another method of choosing the next input is

$$g_{k+1}(x) = \begin{cases} g'_k(x), & x \notin \gamma \\ g_k(x) - \beta g'_k(x), & x \in \gamma \end{cases}$$

The above is referred to as the Hybrid Input-Output algorithm which is an improvement over all the above to avoid the stagnation problem. For this algorithm, if at a given value of x the output remains negative for more than an iteration, the corresponding point in the input continues to grow larger and larger until eventually that output value must go to non-negative.

1.1.5 Additional Methods

Apart from the methods listed above the following other approaches are being used for Image restoration from incomplete data

Restoration by Convex Projections

Using Linear programming

1.2 OVERVIEW

The organisation of this thesis has been made as under

Chapter 1 -Introduction, nature and scope of the problem. Existing algorithms for Phase retrieval from partial information. Alternative Gradient search methods and Iterative Fourier Transform methods are described.

Chapter 2 -The Multiresolution Analyis

Chapter 3 - Phase Retrieval

Chapter 4 -Typical Reconstruction experiments, some practical considerations and results.

Chapter 5 Conclusions and scope for future work.

Chapter 2

The Multiresolution Analysis

An important problem of image processing is to choose a representation that is well adapted for analysing the information content of the images as per the applications. The sharp variations of signal amplitudes are generally among the most meaningful features. The information extraction and analysis is done more often by the decomposition of the image using various transforms. The earliest known such transforms were the Fourier representation. They use the orthogonal properties of the exponential family of basis functions and decompose the signal in terms of harmonic sinusoids. However they are characterised by their uniformity of scales in the time-frequency plane resulting in equal resolution analysis of the signal. When the signal includes structures that justify more close look into certain components of the signal, it is helpful to study the functions which have the microscopic ability and adaptability to say characterise the signals as per their frequency components on different scales. While short time Fourier transform *STFT* to a certain extent does the same signal analysis on a rectangular grid, the sampling of the time-frequency grid with wavelet transforms are very different. Lower frequencies, where the band-

width is narrow (the basis functions are stretched in time) are sampled with larger time steps while the higher frequencies are sampled more often resulting in a constant relative bandwidth as opposed to *STFT*. Hence the wavelet transform is a tool that cuts up data or functions into different frequency components, and then studies each component with a resolution matched to its scale. The wavelets had hence been constructed with a view ideally suited for multiresolution analysis and decomposition.

2.1 Wavelets : A Review

Wavelet transform of a signal implies the decomposition of a signal with a family of orthonormal bases $\psi_{m,n}(x)$; $m, n \in \mathbb{Z}$, obtained through translation and dilation of a kernel function $\psi(x)$ known as the **mother wavelet** i.e.,

$$\psi_{m,n}(x) = 2^{-m/2} \psi(2^{-m}x - n) \quad (2.1)$$

Due to orthonormality, the wavelet coefficients of a signal $f(x)$ can be computed by the analysis formula

$$c_{m,n} = \sum_x f(x) \psi_{m,n}(x) \quad (2.2)$$

To recover the signal from the wavelet coefficients, the synthesis formula is

$$f(x) = \sum_{m,n} c_{m,n} \psi_{m,n}(x) \quad (2.3)$$

2.1.1 Wavelets : Construction

To construct the mother wavelet $\psi(x)$, the scaling function $\phi(x)$ with multiresolution analysis is used. The spaces of square integrable functions $L^2(\mathbb{R})$ is decomposed into

closed subspaces V_{2^m} with the following properties

- $V_{2^m} \subset V_{2^{m-1}}$: The coarser subspaces are contained in the finer one.
- $\cap_{m \in \mathbb{Z}} V_{2^m} = 0$: Separation condition.
- $\overline{\cup_{m \in \mathbb{Z}} V_{2^m}} = L^2(R)$: condition for completeness.
- $f(x) \in V_{2^m} \leftrightarrow f(2x) \in V_{2^{m+1}}$: Scaling property.
- There exists a scaling function $\phi(x) \in V_{2^0}$ such that

$$\phi_{m,n}(x) = 2^{-m/2} \phi(2^{-m}x - n); m, n \in \mathbb{Z} \quad (2.4)$$

- Since $\phi(2x) \in V_{2^1} \subset V_{2^0}$ and $\phi(2x)$ is a basis for the subspace V_{2^1} , the scaling function can be written as a linear combination of $\phi(2x)$ and it satisfies the two scale difference eqn

$$\phi(x) = \sqrt{2} \sum_k h(k) \phi(2x - k) \quad (2.5)$$

The wavelet kernel $\psi(x)$ is given from the scaling function by the equation

$$\psi(x) = \sqrt{x} \sum_k g(k) \phi(2x - k) \quad (2.6)$$

where

$$g(k) = (-1)^k h(1 - k) \quad (2.7)$$

2.1.2 Wavelet Decomposition

To perform wavelet decomposition, a recursive algorithm is implemented. The explicit forms of $\phi(x)$ and $\psi(x)$ are not required as they depend on $h(k)$ and $g(k)$

respectively, given by Eqns., 2.5 and 2.6. A J level decomposition can be written as

$$\begin{aligned} f_0(x) &= \sum_k c_{0,k} \phi_{0,k}(x) \\ &= \sum_k (c_{J+1,k} \phi_{J+1,k}(x) + \sum_{j=0}^J d_{j+1,k} \psi_{j+1,k}(x)) \end{aligned} \quad (2.8)$$

where coefficients $c_{0,k}$ are given and coefficients $c_{j+1,n}$ and $d_{j+1,n}$ at scale $j+1$ are related to the coefficients $c_{j,k}$ at scale j by the equations

$$C_{j+1,n} = \sum_k c_{j,k} h(k - 2n) \quad (2.9)$$

and

$$d_{j+1,n} = \sum_k c_{j,k} g(k - 2n) \quad (2.10)$$

where $0 \leq J$. thus equations 2.9 and 2.10 provide a recursive algorithm for wavelet decomposition through $h(k)$ and $g(k)$ and the final outputs include a set of J level coefficients $d_{j,n}; 1 \leq j \leq J$ and the coefficient $c_{J,n}$ for the low resolution component $\phi_{J,k}(x)$. Similarly the recursive formula for the synthesis of the function is based on the wavelet coefficients $d_{j,n}; 1 \leq j \leq J$ and $c_{J,n}$ such that

$$c_{j,k} = \sum_n c_{j+1,n} h(k - 2n) + \sum_n d_{j+1,n} g(k - 2n) \quad (2.11)$$

Fig. 2.3 illustrates the decomposition given in eqns 2.9 and 2.10. The pair of filters H and G with impulse responses $h(n) = h(-n)$, $g(n) = g(-n)$ are the QMF filters, corresponding to the half band low pass and high pass filters. Fig.2.4 illustrates the reconstruction procedure implemented by upsampling the subsignals c_{j+1} and d_{j+1} (interpolating) and filtering with $h(n)$ and $g(n)$ respectively, and subsequent addition of two signals. The wavelet transform decomposition is performed

recursively at the output of the low pass filter ‘H’. Thus the wavelet transform decomposes a signal into a set of frequency channels that have narrower bandwidths in the lower frequency region.

2.1.3 Two Dimensional Wavelet Decomposition

The wavelet decomposition can be likewise generalised to any dimension $n > 0$. Extending it to two dimensions for image processing, the signal is now a finite energy function $f(x, y) \in L^2(R^2)$. Let $(V_{2^j})_{j \in \mathbb{Z}}$ be the multiresolution approximation of $L^2(R^2)$. The approximation of the signal $f(x, y)$ at a resolution 2^j is equal to its projection on the vector space V_{2^j} . Let V_{2^j} be a separable multiresolution approximation of $L^2(R^2)$. Let $\phi(x, y) = \phi(x)\phi(y)$ be the associated separable two dimensional scaling function. Let $\psi(x)$ be the one-dimensional wavelet associated with the scaling function $\phi(x)$. Then the three wavelets are defined as

$$\begin{aligned}\psi^1(x, y) &= \phi(x)\psi(y) \\ \psi^2(x, y) &= \psi(x)\phi(y) \\ \psi^3(x, y) &= \psi(x)\psi(y)\end{aligned}\tag{2.12}$$

Just as in the one dimensional case, the wavelet decomposition of a two dimensional signal involves convolving the signal with the separable, 2-D scaling function and the three wavelet functions given by equations 2.11. Just as the exact form of the scaling and wavelet functions in the one dimensional case was not required for the decomposition and the QMFs with impulse response $h(n)$ and $g(n)$ were utilised, the 2-D QMF filter coefficients are generated as follows

$$\begin{aligned}h_{LL}(k, l) &= h(k)h(l) \\ h_{LH}(k, l) &= h(k)g(l)\end{aligned}$$

$$\begin{aligned}
h_{HL}(k, l) &= g(k)h(l) \\
h_{HH}(k, l) &= g(k)g(l)
\end{aligned} \tag{2.13}$$

The 2-D wavelet decomposition and reconstruction are illustrated in the Figures 2.5 and 2.6 respectively.

2.2 Multiresolution Analysis: The basic idea

Let $A_{2^j}f(x)$ be the operator which approximates a signal at a resolution 2^j . We suppose that our original signal $f(x)$ is measurable and has finite energy : $f(x) \in L^2(R)$. Here we characterize A_{2^j} from the intuitive properties that one would expect from such an approximation operator:

1. *A_{2^j} is a linear operator* If $A_{2^j}f(x)$ is the approximation operator of some function $f(x)$ at the resolution 2^j , then $A_{2^j}f(x)$ is not modified if we approximate it again at the resolution 2^j . This principle shows that $A_{2^j} \circ A_{2^j} = A_{2^j}$. The operator A_{2^j} is thus a projection operator on a particular vector space $V_{2^j} \subset L^2(R)$. The vector space V_{2^j} can be interpreted as the set of all possible approximations at the resolution 2^j of functions in $L^2(R)$.

2. *Among all the approximated functions at the resolutions 2^j , $A_{2^j}f(x)$ is the function which is most similar to $f(x)$*

$$\forall g(x) \in V_{2^j}, \|g(x) - f(x)\| \geq \|A_{2^j}f(x) - f(x)\| \tag{2.14}$$

Hence, the operator A_{2^j} is an orthogonal projection on the vector space V_{2^j} .

3. *Containment* The approximation of a signal at a resolution 2^{j+1} contains all the necessary information to compute the same signal at a smaller resolution.

This is causality property. Since A_{2j} is a projection operator on V_{2j} this principle is equivalent to

$$\forall j \in \mathbb{Z}, V_{2j} \subset V_{2j+1} \quad (2.15)$$

4. *An approximation operation is similar at all resolutions* The spaces approximated should be thus derived from one another by scaling each approximated operator by the ratio of their resolution values

$$\forall j \in \mathbb{Z}, f(x) \in V_{2j} \Leftrightarrow f(2x) \in V_{2j+1} \quad (2.16)$$

5. *The approximation A_{2j} of a signal $f(x)$ can be characterized by 2^j samples per length unit* When $f(x)$ is translated by a length proportional to 2^{-j} , $A_{2j}f(x)$ is translated by the same amount and is characterized by the same samples which have been translated. As a consequence of para 3, it is sufficient to express this principle for the resolution $j = 0$. The mathematical translations consists of the following

- Discrete characterization. There exists an isomorphism I from V_1 onto $I^2(\mathbb{Z})$.
- Translation of the approximation

$$\forall k \in \mathbb{Z}, A_1 f_k(x) = A_1 f(x - k), \text{ where } f_k(x) = f(x - k) \quad (2.17)$$

- Translation of samples

$$I(A_1(f(x))) = (\alpha_i)_{i \in \mathbb{Z}} \Leftrightarrow I(A_1(f_k(x))) = (\alpha_{i-k})_{i \in \mathbb{Z}} \quad (2.18)$$

6. When computing an approximation of $f(x)$ at resolution 2^j , some information about $f(x)$ is lost. However as the resolution increases to $+\infty$ the approximated signal should converge to the original signal. Conversely as the resolution

decrease to zero, the approximated signal contains less and less information and converges to zero.

Since the approximated signal at resolution 2^j is equal to the orthogonal projection on a space V_{2^j} , this principle can be written as

$$\lim_{j \rightarrow +\infty} V_{2^j} = \bigcup_{j=-\infty}^{+\infty} V_{2^j} \text{ is dense in } L^2(R) \quad (2.19)$$

and

$$\lim_{j \rightarrow -\infty} V_{2^j} = \bigcap_{j=-\infty}^{+\infty} V_{2^j} \quad (2.20)$$

We call any set of vector spaces which satisfies the above properties, the *multiresolution approximation* of $L^2(R)$.

It has been seen that the approximation operator A_{2^j} is an orthogonal projection on the vector space V_{2^j} . In order to numerically characterize this operator, we must find an orthonormal basis of V_{2^j} . Theorem 3.1 shows that such an orthogonal basis can be defined by dilating and translating a unique function $\phi(x)$.

Theorem 3.1 Let $(V_{2^j})_{j \in \mathbb{Z}}$ be a multiresolution approximation of $L^2(R)$. There exists a unique function $\phi(x) \in L^2(R)$, called *scaling function*, such that if we set $\phi_{2^j}(x) = 2^j \phi(2^j x)$ for $j \in \mathbb{Z}$ (the dilation of $\phi(x)$ by 2^j), then

$$\left(\sqrt{2^{-j}} \phi_{2^j}(x - 2^{-j} n) \right)_{n \in \mathbb{Z}} \quad (2.21)$$

is an orthonormal basis of V_{2^j} . For proof of above ref. [3]. The theorem shows that an orthonormal basis of any V_{2^j} can be built by dilating a function $\phi(x)$ with a coefficient 2^j and translating the resulting function on a grid whose interval is proportional to 2^{-j} . The functions $\phi_{2^j}(x)$ are normalized with respect to the $L^1(R)$ norm. The coefficient $\sqrt{2^{-j}}$ appears in the basis set in order to normalize the functions in the $L^2(R)$ norm. For a given multiresolution approximation $(V_{2^j})_{j \in \mathbb{Z}}$, there exists

a unique scaling function $\phi(x)$ which satisfies the above equation. However, for different multiresolution approximation, scaling functions are different.

The orthogonal projection on V_2 , can now be computed by decomposing the signal $f(x)$ on the orthonormal basis given by Theorem 3.1. That is,

$$\forall f(x) \in L^2(R), A_{2^j} f(x) = 2^{-j} \sum_{n=-\infty}^{+\infty} \langle f(u), \phi_{2^j}(u - 2^{-j}n) \rangle \phi_{2^j}(x - 2^{-j}n) \quad (2.22)$$

The algorithm for determining *discrete approximation* to the signal $f(x)$ at resolution 2^j can be found as Mallat's decomposition algorithm in [3]. Since $\phi(x)$ is a low pass filter, this discrete signal can be interpreted as low pass filtering of $f(x)$ followed by uniform sampling at the rate 2^j . The scaling function $\phi(x)$ forms a very special low pass filter since the family of functions $(\sqrt{2^{-j}} \phi_{2^j}(x - 2^{-j}n))_{n \in \mathbb{Z}}$ is an orthonormal family.

Before we consider the wavelet representation, it will be pertinent to list one more useful theorem as under(for proof ref [3])

Theorem 3.2 Let $\phi(x)$ be a scaling function, and let H be a discrete filter with impulse response $h(n) = \langle \phi_{2^{-1}}(u), \phi(u-n) \rangle$. Let $H(\omega)$ be the Fourier transform defined as

$$H(\omega) = \sum_{n=-\infty}^{+\infty} h(n) e^{-in\omega} \quad (2.23)$$

$H(\omega)$ satisfies the following two properties:

$$|H(0)| = 1 \text{ and } h(n) = O(n^{-2}) \text{ at } \infty \quad (2.24)$$

$$|H(\omega)| + |H(\omega + \pi)|^2 = 1 \quad (2.25)$$

Conversely let $H(\omega)$ be a Fourier transform satisfying above equations and such that

$$|H(\omega)| \neq 0 \text{ for } \omega \in [0, \pi/2] \quad (2.26)$$

The function defined by

$$\hat{\phi}(\omega) = \prod_{p=1}^{\infty} H(2^{-p}\omega) \quad (2.27)$$

is the Fourier transform of the scaling function.

Our aim here is to build a multiresolution representation based on the difference of information available at two successive resolutions 2^{j+1} and 2^j . This difference of information is called the *detail signal* at the resolution 2^j . The approximation at the resolution 2^{j+1} and 2^j of the signal are respectively equal to its orthogonal projection on $V_{2^{j+1}}$ and V_{2^j} . By applying the projection theorem, we can easily show that the detail signal at the resolution 2^j is given by the orthogonal projection of the original signal on the orthogonal complement of V_{2^j} in $V_{2^{j+1}}$. Let O_{2^j} be this complement, i.e., O_{2^j} is orthogonal to V_{2^j} ,

$$O_{2^j} \oplus V_{2^j} = V_{2^{j+1}} \quad . \quad (2.28)$$

To compute the orthogonal projection of a function $f(x)$ on O_{2^j} , we need to find an orthonormal basis of O_{2^j} . Next theorem shows that such a basis can be built by scaling and translating a function $\psi(x)$.

Theorem 3.3 Let $(V_{2^j})_{j \in \mathbb{Z}}$ be a multiresolution vector space sequence, $\phi(x)$ the scaling function, and H the corresponding conjugate filter. Let $\psi(x)$ be a function whose Fourier transform is given by

$$\hat{\psi}(\omega) = G\left(\frac{\omega}{2}\right) \hat{\psi}\left(\frac{\omega}{2}\right); G(\omega) = e^{-i\omega} \overline{H(\omega + \pi)} \quad (2.29)$$

Let $\psi_{2^j}(x) = 2^j \psi(2^j x)$ denote the dilation of $\psi(x)$ by 2^j then $(\sqrt{2^{-j}} \psi_{2^j}(x - 2^{-j}n))_{(n,j) \in \mathbb{Z}^2}$ is an orthonormal basis of O_{2^j} and $(\sqrt{2^{-j}} \psi_{2^j}(x - 2^{-j}n))_{(n,j) \in \mathbb{Z}^2}$ is an orthonormal basis of $L^2(\mathbb{R})$. $\psi(x)$ is called an orthogonal wavelet.

We have hence seen that as $\phi_{j,k}, K \in \mathbb{Z}$ is the orthonormal basis for V_{2^j} , any function belonging to $L^2(\mathbb{R})$ can now be decomposed along all translates of $\phi(2^j x)$.

The result is denoted by $A_{2^j}^d$. Similarly the function can be decomposed along all translates of $\psi(2^j x)$ and the result is denoted by $D_{2^j}^d$. If the actual signal is having N number of samples these results are having $N/2^j$ number of samples. Thus the resulting signals belong to $L^2(N/2^j)$.

The decomposed signal along all the translates of $\phi(2^j x)$ is called the averaging signal and the decomposed signal along all the translates of $\psi(2^j x)$ is called the detail signal. This is due to the nature of finite sequences $h(n)$ and $g(n)$ used to generate the $\phi(x)$ and $\psi(x)$ respectively.

2.3 Quality Criterion For Wavelets Used In Image Processing

Before choosing a wavelet for a particular application some essential quality criterion needs to be mentioned which characterise each type of wavelets [9]

Wavelet regularity The regularity of the mother wavelet is important and appears to be closely related to the regularity of the signals to be processed. Since images are generally *smooth* to the eye, with the exception of occasional edges, it is appropriate to use regular wavelets. Indeed, there is a trade-off between wavelet regularity and the visual effect on the processed images. Because scaling function $\phi(t)$ and the wavelet function $\psi(t)$ are related, they share the same regularity. Therefore in this discussion we restrict ourselves to the study of $\phi(t)$, which depends only on low pass filter $H(z)$. Zeros at the Nyquist frequency play an important role in determining the regularity. One zero in $H(z)$ at $z = -1$ is necessary to obtain continuity. To achieve regularity order

of N , $H(z)$ must have atleast $N + 1$ zeros at $Z = -1$. However if other *zeros* are also present, then they contribute towards *killing* the effect of regularity caused by zeros at $z = -1$. This effect can be as much as 90%. This has been studied earlier and an algorithm to estimate the optimal regularity estimate is existing. The same is reproduced below:

1. Remove all the zeros of $H(z)$ at $z = -1$. These zeros will contribute to a maximum Holder regularity of K , the actual number of zeros at $z = -1$.
2. The remaining factor $F(z) = (1 + z^{-1})^{-K} H(z)$ will decrease this regularity. The decrease will be by the amount $1 - \alpha$.
3. α , mentioned above is calculated by first iterating $F(z)$ as under:

$$F^i(z) = F(z)F(z^2) \dots F(z^{2^{i-1}})$$

Associated with this $F^i(z)$, we have time sequence f_n^i . Then, α_i is calculated as under:

$$\alpha_i = 1/i \log_2 \max_n \sum_k |f_{n+2^i k}|$$

4. Regularity r is then given by

$$r = K - 1 + \alpha_i \quad (2.30)$$

In Practice, i is iterated 20 times to get the regularity estimate. In general higher regularity of wavelets give better and tighter constraints.

Vanishing moments It is the oscillatory character of the wavelet and is given in numbers N . For a wavelet $\psi(x)$ it is defined as

$$\sum x^n \psi(x) = 0 \quad \forall n = 0, 1, \dots, N - 1 \quad (2.31)$$

Since ψ is a wavelet, N is greater than or equal to 1 and, the property of the wavelets, where $\sum_x \psi(x) = 0$ is verified. In fact, this property of number of

of vanishing moments is related to the regularity of the wavelet. That is, any r -regular multiresolution analysis of the wavelet will generate ψ with $r + 1$ vanishing moments. Also, all derivatives of $\psi(\omega)$ upto the order $N - 1$ are zero at the point $\omega = 0$. A wavelet with N vanishing moments enables the cancellation of all wavelet coefficients of a polynomial signal whose degree is less than N . Thus, if f is a polynomial signal of degree less than N , on support of $\psi_{m,n}$ then

$$c_{m,n}(f) = \langle f, \psi_{m,n} \rangle = 0 \quad (2.32)$$

Scaling function Spatial characterisation of the scaling function in terms of moments which determine how $\phi(x)$ evolves with respect to x , which allows us to determine the energy concentration of ϕ and provides information on the spatial length or the localisation of ϕ is another significant aspect which needs mention. We introduce the criterion m_k which allows us to characterise the scaling function ϕ spatially. To define m_k , we introduce the function $p(x)$ such that

$$p(x) = \frac{|\phi(x)|^2}{\int |\phi(x)|^2 dx} \quad (2.33)$$

with $p(x) \geq 0$ and $\int p(x)dx = 1$. m_k is then defined as

$$m_k = \int (x - m_1)^k p(x) dx \text{ with } m_1 = \int x p(x) dx \quad (2.34)$$

Thus m_1 is equal to the mathematical expectation of $p(x)$ and m_2 corresponds to the spatial variance of the scaling function ϕ . m_2 allows us to determine the energy concentration of ϕ and provides information on the spatial length or localisation of ϕ . This criterion also apply to the wavelet $w(t)$.

Characterisation of the associated filters To avoid distortion in image processing, the filter $H(\omega)$ associated with the scaling function ϕ must be linear phase or ideally zero phase. Indeed, non-linear phase filters degrade edges

and are more difficult to implement than linear phase filters. The number of elements making up the impulse response of $h(n)$ must be small in order to limit the number of convolutions operations to be performed in the analysis/reconstruction algorithm. It corresponds to wavelets whose support is compact (making the wavelet well localised).

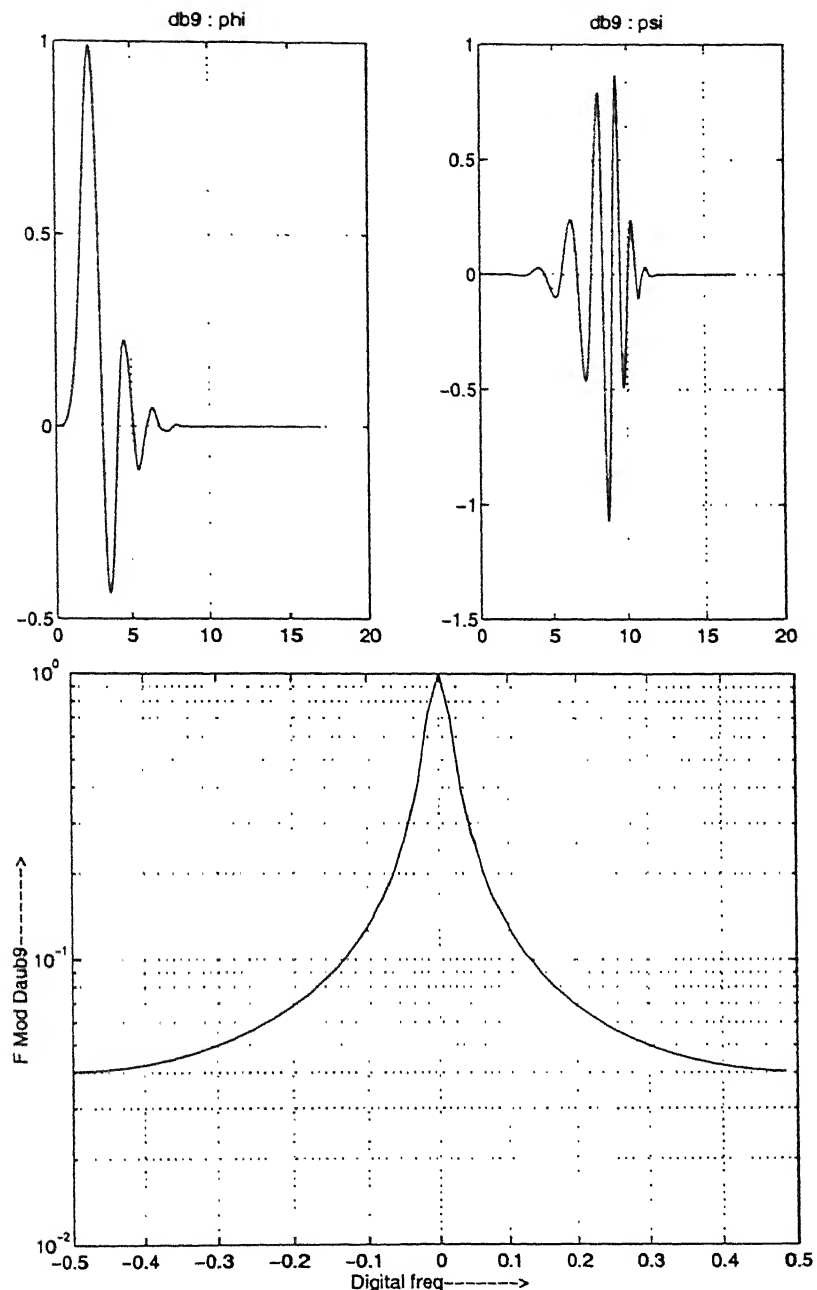


Figure 2.1: Illustration of a Wavelet and their corresponding Scaling Function. Also illustrated is the Fourier modulus of the scaling function. Wavelet is a band pass filter.

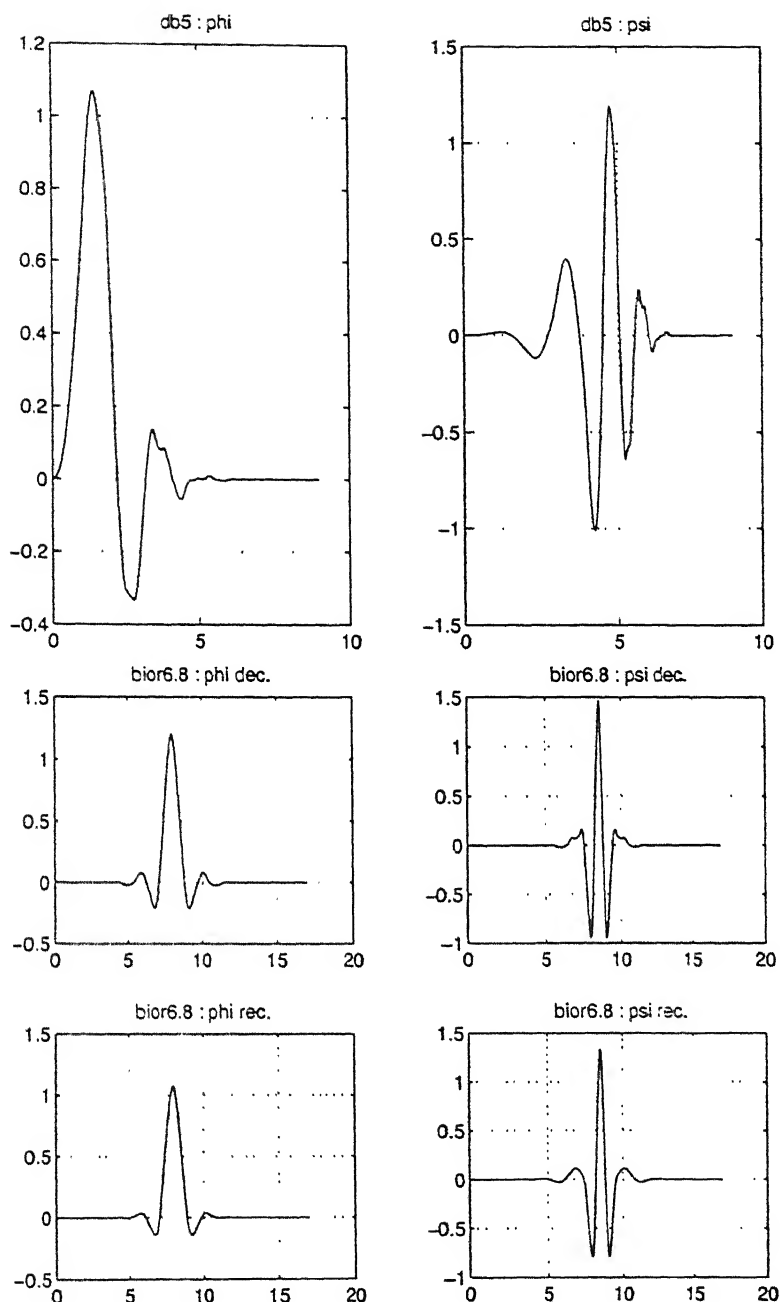


Figure 2.2: Illustration of an orthogonal and a biorthogonal Wavelet and their corresponding Scaling Functions

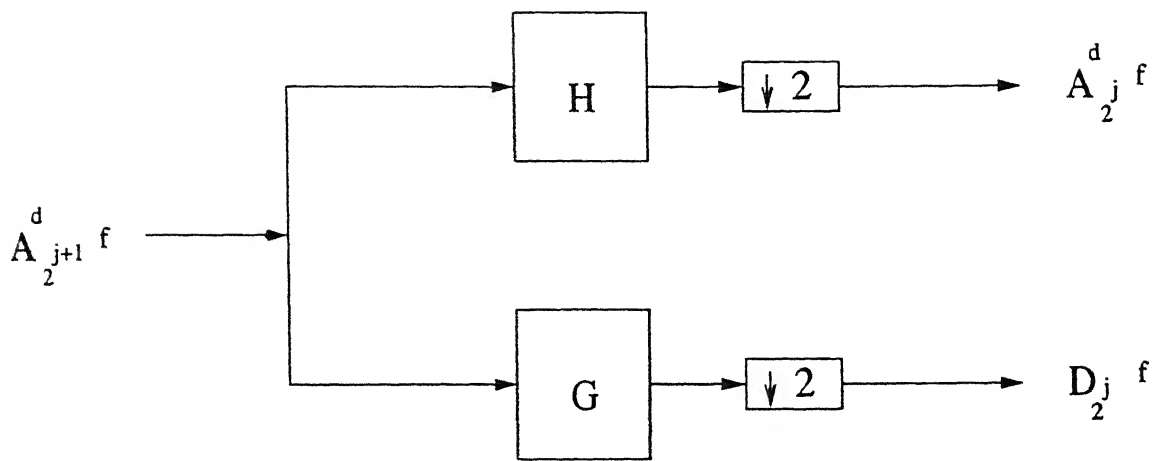


Figure 2.3: Wavelet Decomposition

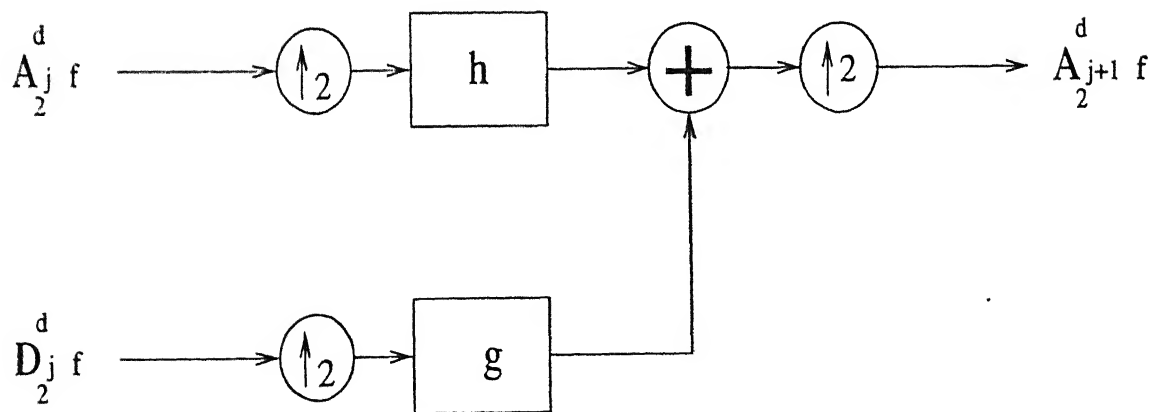


Figure 2.4: Wavelet Reconstruction

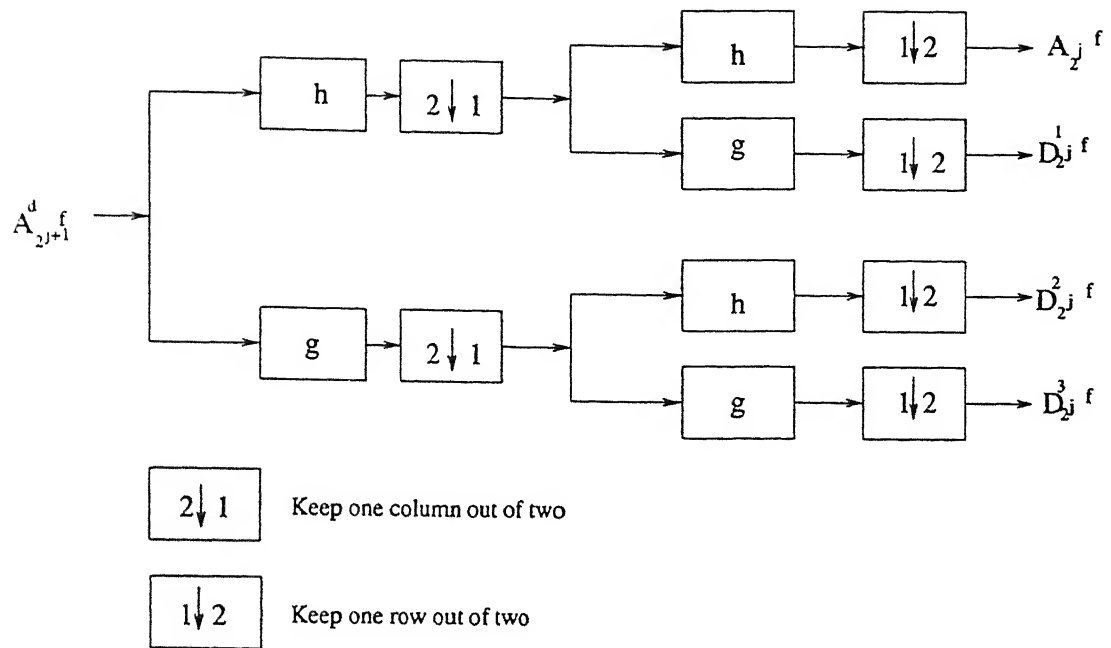


Figure 2.5: 2-D Wavelet Decomposition

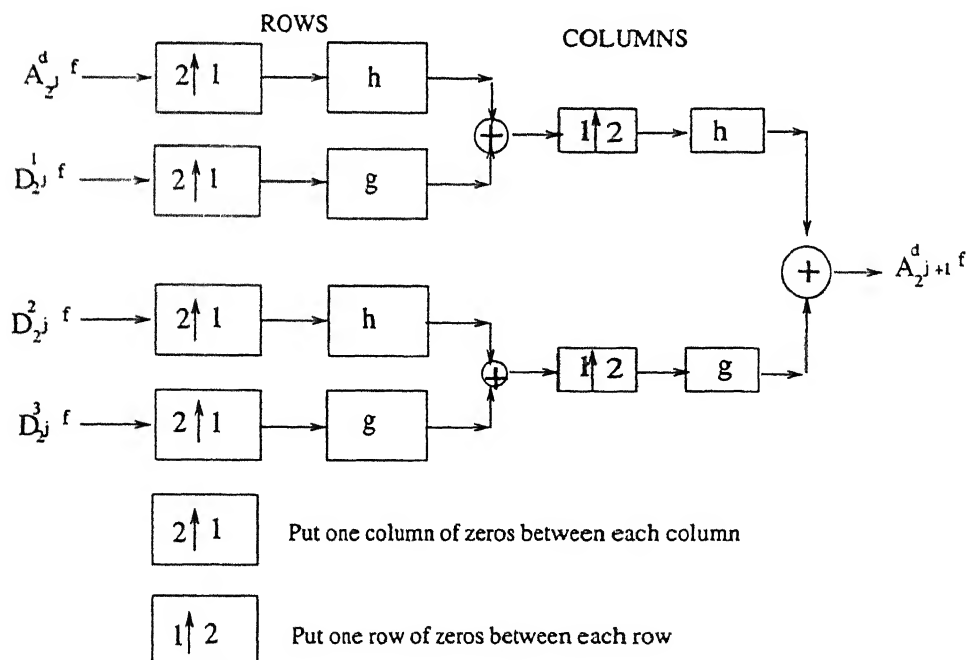


Figure 2.6: 2-D Wavelet Reconstruction

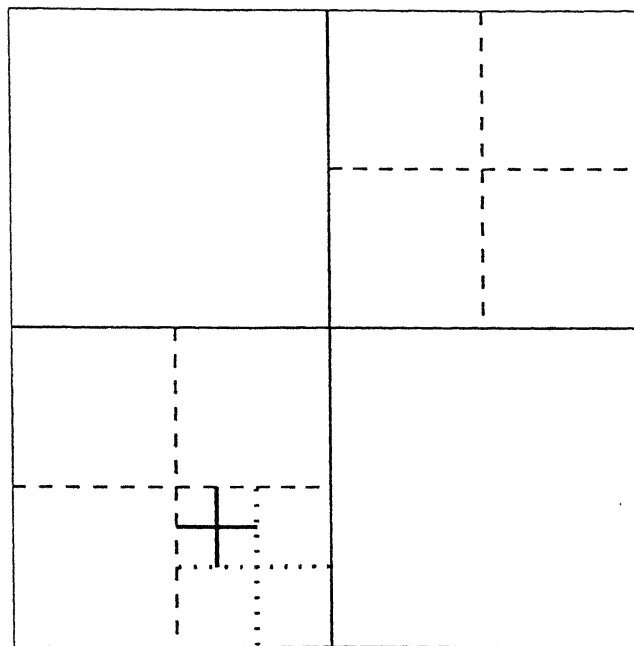


Figure 2.7: Decomposition Of A Two Dimensional Signal Down To Level 4

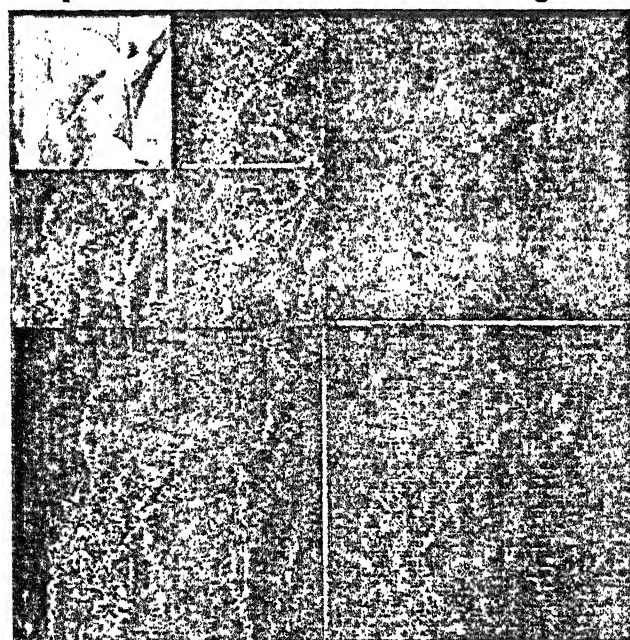


Figure 2.8: Illustration of wavelet decomposition of an Image down to two levels

Chapter 3

Phase Retrieval

3.1 Introduction

The issue which is addressed in this chapter concerns the actual reconstruction of a multidimensional sequence from its Fourier modulus. It has been brought out in earlier chapters that in the absence of any *a priori* additional knowledge of the desired sequence there is as yet no practical algorithm which will always recover the correct phase from only magnitude information. Nevertheless, the Iterative Transform Algorithm has been discussed as also the Wavelet decomposition approach in solving the phase retrieval problem. Three different classes of images have been utilised for the same to investigate robustness of the procedures and results.

Multiresolution analysis concerns itself with decomposing the signal spaces into subspaces using suitable wavelet bases, the quality criterion of which is to be considered for suitability in a certain application. Compactness, regularity and number of Vanishing moments play certain role in determining the efficacy of the

wavelet chosen for a certain task. To this effect many different length wavelet coefficients have been used for multiresolution analysis. Also investigation for wavelets of three different classes have been carried out namely Haar, Daubachies and B-Spline Biorthogonal to see their effect on reconstruction quality. An effective tool during image compression and transmission would be the redundancy in the reconstructed image which have been checked in terms of truncation of Fourier coefficients of the reconstructed image. Low frequency component of the error responsible for the slow convergence of the iterative transform algorithm was another aspect which needed to be studied and therefore to broaden the picture it was seen as to the effect different wavelet quality criterion have on this aspect and their effect on convergence and quality of reconstruction.

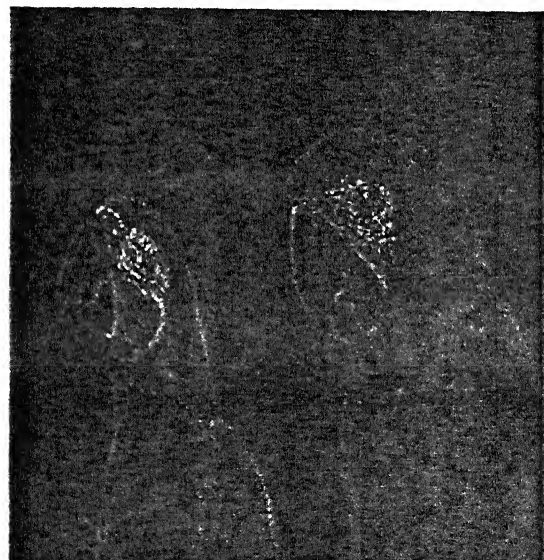
3.2 Fourier synthesis from partial information: Importance of phase

In this section we look at the importance of phase given an incomplete characterisation of the Fourier domain. In particular, we will examine the the effect of combining the phase information with an estimate of magnitude function and the effect of combining magnitude information with an estimate of the phase information. Also the results obtained from coarse quantisation of the phase function will be investigated.

It has been observed in a number of different contexts and applications that many of the important features of a signal are represented in the phase of its Fourier transform [2]. Specially, it is well known that a *phase-only synthesis* of a signal, formed by combining the phase of the Fourier transform of the signal



(a)



(b)

Figure 3.1: Phase only synthesis (a) original image and (b) the image synthesised using complete phase information and constant magnitude function

with either a constant or an ensemble averaged magnitude, contains a number of similarities to the true signal. From the reconstruction experiments performed on the test images reproduced in the figures[3.1]-[3.6] these are established conclusively. Shown in figure 3.1(a) for example is an original image and in Fig. 3.1(b) is the image formed by combining the phase of the Fourier transform of the image with a constant magnitude.

$$y(m, n) = \mathcal{F}^{-1}[\exp\{j\phi_x(\mu, \nu)\}]$$

On the contrast comparing this with a correct magnitude combined with zero Fourier phase(figure 3.4)image establishes that the essence of the image is preserved in the phase of the image only.An even better phase-only synthesis may be obtained, however, by combining the phase of the Fourier transform of the image with a magnitude function which is *more representative* of images.

Although much of the useful information in a signal appears to be represented in the phase of its Fourier transform, the phase-only synthesis assumes perfect phase information. Yet it has been observed that even with a coarsely quantised representation of the phase, a reasonable synthesis may be obtained and the reconstructed image contains lot of similarities to the original as compared to the unknown phase.The same is being established with the help of test images(Figures 3.2, 3.3). The one bit phase function is given by

$$Q[\phi(\mu, \nu)] = \begin{cases} 0 & \text{if } |\phi(\mu, \nu)| \leq \pi/2 \\ \pi & \text{otherwise} \end{cases}$$

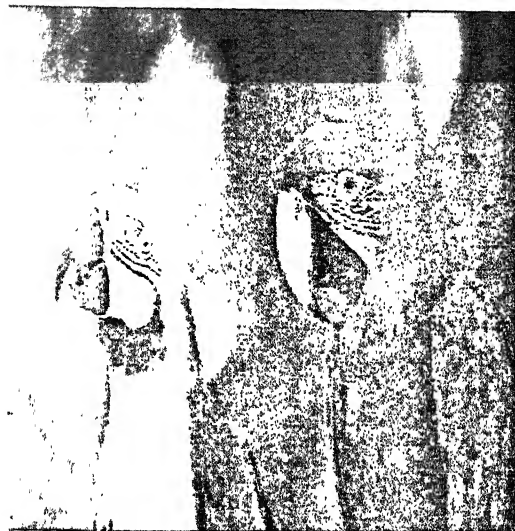
As a result, the phase-only synthesis is simply given by

$$y(m, n) = \mathcal{F}[Y(\mu, \nu)]$$

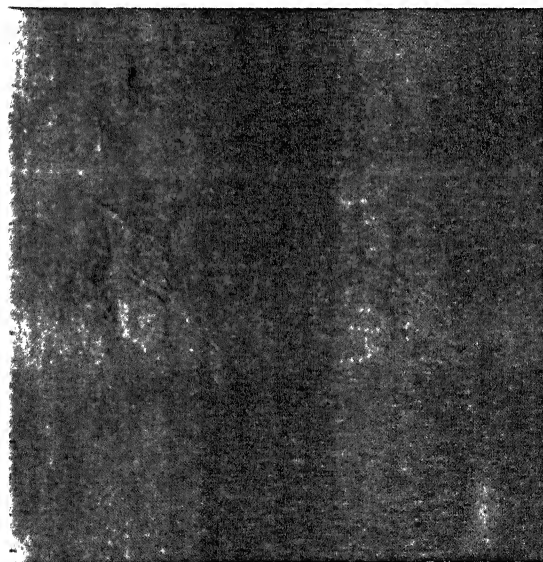
where

$$Y(\mu, \nu) = \begin{cases} 1 & \text{if } |\phi(\mu, \nu)| \leq \pi/2 \\ -1 & \text{otherwise} \end{cases}$$

256x256 BIRD ORIGINAL



(a)

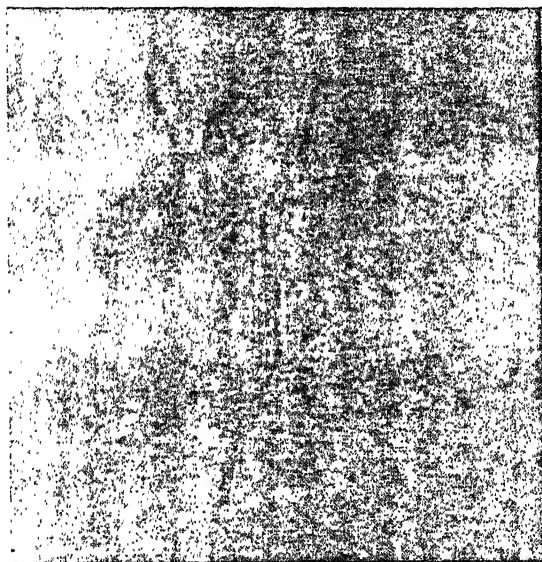


(b)

Figure 3.2: Magnitude only synthesis (a) original image and (b) the image synthesised using complete magnitude information and 1-bit phase function



(a)



(b)

Figure 3.3: Magnitude only synthesis (a) original image and (b) the image synthesised using complete magnitude information and 1-bit phase function

An improved synthesis may be obtained by an ensemble averaged magnitude function(as opposed to constant) which is obvious.

Having observed the importance of phase information in the representation of images, it will be worthwhile to investigate the relative importance of magnitude information in signal representation. Therefore a set of experiments similar to those listed above were also performed to examine the importance of magnitude information. Shown in fig 3.4, for example , is an original image, $x(m, n)$, and shown alongside is a magnitude-only synthesis formed by combining the magnitude of the Fourier transform of $x(m, n)$ with zero phase

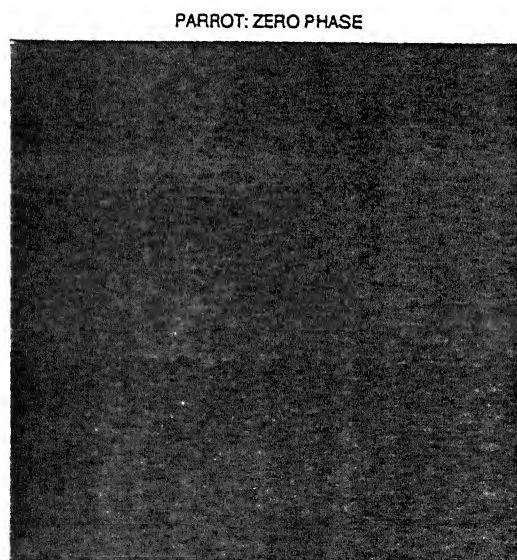
$$y(m, n) = \mathcal{F}[|X(\mu, \nu)|]$$

Clearly, there is no useful information portrayed with this synthesis. Also experimented was the combination of the magnitude of the Fourier transform of $x(m, n)$ with the phase of another image (figures 3.5 and 3.6). As expected, the image produced by this synthesis bears a resemblance to the image whose Fourier phase was used.

The conclusion to be drawn from the above set of investigations are that there is, apparently, a significant amount of information conveyed in the phase of the Fourier transform of signals, which makes the phase retrieval problem very significant.



(a)



(b)

Figure 3.4: Magnitude only synthesis (a) original image and (b) the image synthesised using complete magnitude information and zero phase function

256x256 CAMERAMAN ORIGINAL



(a)



(b)

Figure 3.5: Magnitude only synthesis (a) original image and (b) the image synthesised using complete magnitude information of cameraman image and phase function from bird image



Figure 3.6: Magnitude only synthesis shows magnitude information of bird image and phase function from cameraman image

3.3 Phase retrieval problem : The uniqueness question

In this section we consider the reconstruction problem of a $2 - D$ signal in the background of the uniqueness of reconstruction. It has been mentioned earlier that without any additional constraints or information apart from magnitude information, a signal is not uniquely specified by the magnitude of its Fourier transform [4]. For example, a signal may always be shifted (delayed) or multiplied by a factor of -1 without changing the magnitude of its Fourier transform. Thus, any signal $y(m, n)$ which is related to $x(m, n)$ by

$$y(m, n) = \pm x(m + k, n + l)$$

for any integers k and l has a Fourier transform with the same magnitude as $x(m, n)$. In addition, rotating a signal by 180° [or reflection about the point $(0, 0)$] will not change the magnitude of its Fourier transform, so $x(m, n)$ and

$$y(m, n) = x(-m, -n)$$

have the same Fourier magnitude. In most applications, perhaps these ambiguities are of no concern since it is the relative amplitudes of the various samples within the signal that are of primary importance. Therefore although such reconstructions have been observed in many reconstructions in this thesis, yet two signals $x(m, n)$ and $y(m, n)$ will be said to be *equivalent* as per convention if they are related to one another by any combination of the above relations. Excluding this ambiguities, it is still not possible to uniquely define a signal in terms of its spectral magnitude because of the following:

- It is always possible to convolve a signal with an arbitrary *all-pass* signal (say one which has a Fourier transform with unit modulus also) to obtain another signal with the same spectral magnitude.

3.3.1 Uniqueness :Revisited

Having said, that without any additional information or constraints a signal is not generally defined by the magnitude of its Fourier transform, with only the finite length constraint, we state that due to the irreducibility of almost all polynomials in two or more variables, an important conclusion can be drawn from the uniqueness theorem [4], [2]. In particular it has been shown in the above theorem that a 2-D signal with finite support which has an irreducible z -transform is uniquely defined (to within a sign, time shift, and time reversal) by the magnitude of its Fourier

transform. Although this theorem assumes that the Fourier magnitude is known for all frequencies, yet this can be generalised to show that uniqueness still holds if the magnitude of the DFT of $x(m, n)$ is known.

3.4 Direct Approach: The Fienup Algorithm

The image reconstruction problem (also known as *phase retrieval* problem) can be stated as follows:

Given the magnitude of the Fourier transform, $|F(u, v)|$, of a bandlimited image $f(x, y) \in L^2(R)$, and some apriori information on $f(x, y)$, reconstruct the image $f(x, y)$, or equivalently, retrieve the phase $\Phi(u, v)$ of $F(u, v)$.

To this effect the Fienup algorithm was chosen due to its wide acceptability and practicability. It was supposed that the image Fourier modulus was the only information given and any other apriori information was assumed as not available.

The Fienup algorithm is based on the idea that by iterating between the spatial and frequency domains and successively enforcing the known constraints at each stage one can obtain a numerical solution that minimizes the distance between the measurement and its estimate. For the most general problem the Fienup algorithm consists of the following four steps (for the k th iteration)

1. Fourier transform $g_k(x, y)$, an estimate of $f(x, y)$, yielding $G_k(u, v)$
2. Make the minimum changes in $G_k(u, v)$ which allow it to satisfy the Fourier-domain constraints to form $G'_k(u, v)$, an estimate of $F(u, v)$
3. Inverse Fourier transform $G'_k(u, v)$, yielding $g'_k(x, y)$, the corresponding image

4. Make the minimum changes in $g'_k(x, y)$ that allow it to satisfy the object domain constraints to form $g_{k+1}(x, y)$, a new estimate of the object.

For phase retrieval for a non negative object from the Fourier modulus $|F(u, v)|$, these four steps are

$$1. G_k(u, v) = |G_k(u, v)| \exp[i\phi_k(u, v)] = \mathcal{F}[g_k(x, y)]$$

$$2. G'_k(u, v) = |F(u, v)| \exp[i\phi_k(u, v)]$$

$$3. g'_k(x, y) = \mathcal{F}^{-1}[G'_k(u, v)]$$

$$4. g_{k+1}(x, y) = \begin{cases} g'_k(x, y), & (x, y) \notin \gamma \\ 0, & (x, y) \in \gamma \end{cases}$$

Where γ is the set of points at which $g'_k(x, y)$ violates the object-domain constraints and where g_k , and G'_k , and ϕ_k are estimates of f , F , and the phase ψ of F , respectively.

The algorithm was started by using an array of random numbers uniformly distributed between 0 – 255 assuming an 8-bit format for further image processing. In this thesis as has been mentioned earlier the step four of the algorithm has been modified as per Hybrid Input-Output algorithm for getting better stagnation profile during reconstruction. Hence the step 4 has been taken as under:

$$g_{k+1}(x, y) = \begin{cases} g'_k(x, y), & (x, y) \notin \gamma \\ g_k(x, y) - \beta g'_k(x, y), & (x, y) \in \gamma \end{cases}$$

Where β is a constant feedback parameter which controls the level of change in the next iteration updated guess. Values of β can vary between 0.5 to 1. For this thesis the value of β as 0.7 worked well and was hence fixed for all reconstructions.

In practice a number of cycles of iterations were performed, where one cycle consisted of, 40 – 50 iterations of the Hybrid Input-Output algorithm followed by 5 – 10 iterations of the basic Fienup algorithm.

For the general images including astronomical images (Available 8-bit 128 × 128 data of *Saturn* taken by Hubble space telescope was used as a test case), the object domain constraints are the objects nonnegativity and a (usually loose) support constraint. Then the points in the set γ are those outside the assumed support and those within the support for which $g'_k(x, y) < 0$. The diameter of the object was estimated since it is just half the diameter of the autocorrelation. However it is evident that such estimation is only rough and the exact support of the object cannot be determined uniquely from the support of the autocorrelation and so the support constraint cannot be applied tightly. At best the support can be subsequently used for cleaning up the image if satisfactory reconstruction has been obtained in the first run. Computational expense has to be however kept in mind for such inadequate support constraints.

3.4.1 Convergence for the algorithm

A measure of convergence of the algorithm to a solution(a Fourier transform pair satisfying all the constraints in both domains) is the normalised root-mean-squared (NRMS) error metric in the Fourier domain:

$$F_F = \left[\frac{\sum_u \sum_v [|G(u, v)| - |F(u, v)|]^2}{\sum_u \sum_v |F(u, v)|^2} \right]^{1/2} \quad (3.1)$$

or in the object domain,

$$E_0 = \left[\frac{\sum \sum_{(x,y) \in \gamma} |g'_k(x, y)|^2}{\sum_y \sum_y |g'_k(x, y)|^2} \right]^{1/2} \quad (3.2)$$

where γ is defined as earlier. The summations are performed over all points in image or Fourier space. Since the convergence of the algorithm with little known constraints is usually slow, it is only natural that error be noted only after atleast one cycle of iterations comprising of say total 40 – 100 iterations of the Fienup algorithm.

3.4.2 Additional aspects of the Fienup algorithm

Most often the Fienup algorithm will give a reasonable image reconstruction and when the error goes down to within limits of visual satisfaction, one can think that the solution has been found. Alternatively as the error starts stagnating for atleast 3-4 cycles than one can assume that the reconstruction is trapped in a minima. It is unlikely that error will ever go to zero because(apart from others)

1. The Fourier modulus resolution may not be satisfactory to resolve the reconstruction.
2. Tight or incorrect support constraint makes the reconstruction inconsistent with either the nonnegativity constraint or the Fourier modulus.
3. Choice of initial input to the algorithm varies the error profile as has been observed [4]

For the general problem one has a nonnegativity constraint in the object domain. Furthermore one can compute the bounds on the support of the object from the autocorrelation which roughly resembles that of the object if the Fourier modulus resolution is sufficient. The simplest way is to use a rectangle that is half the size, in each dimension, of the smallest rectangle that encloses the autocorrelation.

Actual support of the object has been considered to be not known in our case and thresholding of autocorrelation to .005 of the maximum value has been used to find a support mask. The support mask has been defined as a mask which is unity inside the support and zero outside. In effect the autocorrelation is thresholded to .005, demagnified by a factor of 2 in each dimension by discarding every other row and column and filled up with ones to construct a mask.

There are many ways to pick an initial estimate as an input to the algorithm [2] and it has been established that although same crude phase estimation methods may have worked with some reconstruction problems but the efficacy has not been established for all. On the other hand it has been found that random numbers perform as well. In case some other known apriori information about the nature of phase is there then that should be used since having an initial input close to the true solution not only reduces the computational complexity but helps to reduce the inevitable stagnation problems. To give the algorithm an unbiased start in the absence of any other information, random numbers were therefore chosen as the initial input in the object domain(alternatively in the Fourier domain, random phase could have been chosen).

The algorithm can be made to converge faster and avoid a stagnation problem if the support mask is chosen to be somewhat smaller than the correct support for the first few cycles. Since it is the incorrect support, the smaller support mask is inconsistent with Fourier modulus and stagnation eventually occurs. Nevertheless, the smaller support mask helps to force most of the energy of the output, $g'(x, y)$, into a confined region in fewer iterations. After this has happened the support mask should be enlarged to the correct support constraint as given by the known or estimated value. During the last few cycles or alternatively if stagnation occurs(error is being computed at the end of each cycle), it is beneficial to enlarge the support mask

to larger values to give *breathing space* to the reconstructed image. In addition it helps since recall that the reconstruction is always having the trivial ambiguities (of translation and reversal) and therefore the support mask often starts hurting the reconstruction by the way of truncating the partially reconstructed image inadvertently. Keeping all these factors in mind, the algorithm was tested with an adaptive mask which increased every four cycles. Satisfactory reconstruction error, stagnation profile and visual quality were hence obtained.

The discrete Fourier transforms are computed with the FFT algorithms. The sampling in the Fourier domain should be fine enough to ensure that the object domain array size is atleast twice the dimensions of the object itself, which is equivalent to achieving the Nyquist sampling rate for $|F(u, v)|^2$.

A practical method of implementation of the algorithm is to compute the phase from the real and imaginary parts of $G_k(u, v)$, then combine it with $|F(u, v)|$ to form $G'_k(u, v)$, and finally compute the real and imaginary parts of $G'_k(u, v)$ (which are required by the FFT) from its modulus and phase.

Depending on the many factors listed above the Fienup algorithm converges to some solution and in some cases requires some additional inputs. The test case of 'Claire' image was one such experiment which did not give a reasonable reconstruction. Apparently the Fourier resolution was not adequate to resolve the details and hence the outline of the image was only visible along with some poor visibility inside the body of the image. It seems increasing the Fourier resolution only marginally helps the reconstruction and there are classes of image which are difficult to reconstruct. Additionally among others, one reason for such poor reconstruction could be the absence of the detail coefficients in the reconstruction which are responsible for blurring of the edges.

Some other problems of reconstruction and stagnation has been adequately documented in literatures [2], examples of which are

- Appearance of simultaneous twin images in reconstruction.
- Superimposed stripes on reconstruction.

However these problems were not encountered in the test cases taken in this thesis.

3.5 Wavelet method :The Multiresolution approach

A major factor in the non convergence of the Fienup algorithm and other related iterative transform algorithms is the choice of the initial input to the algorithms. In general it is known that the closer the initial input is to the true image, the better will be the convergence and subsequent less chances of stagnation. Another major disadvantage in the iterative methods in general is the intensive computational requirements of the pair of 2-D DFTs required at each iterations of a cycle of the algorithm. Since the iterative transform method operates only on a fine grid, the computational complexity is enormous and any saving on this part should be investigated. The wavelet decomposition approach can significantly improve the performance of these algorithms in most of the cases in which reconstruction is generally obtainable from the *Direct methods*. In so far as the visual reconstruction quality is concerned, it was found that a marginal improvement in error profile does not apparently improve the image quality; which may also be due to the limitation of the eyes to discern. Nevertheless it is conclusive that more the input estimate is closer to the true image, the better should be the *chances* of an improved construction. As has been mentioned earlier the quality of reconstruction, the error profile

and the stagnation profile, all depend on the initial input in some way or other, the interrelationship between them is not clearly understood. This results in an even increased error in a few instances at some cycle of iterations vis-a-vis the class of the image. Mention of such instances has also been found in literatures [6]. Nevertheless the multiresolution wavelet approach provides a rough (and quick) estimate of the solution at a low resolution that is later refined employing *coarse to fine* strategy. Following advantages accrue out of this approach:

1. Enables the algorithm to avoid stagnation by providing a better initial guess.
2. Improving the convergence rate by decomposing the search space into orthogonal subspaces and therefore reduction of low frequency component of the error responsible for the slow convergence of the algorithm.
3. Reduction in computational complexity since the number of variables to be estimated at the coarser level is lesser than that at full resolution grid.

3.5.1 The algorithm

Let $f(x)$ be a signal with finite support and let A_m be the operator that approximates a signal $f(x)$ at resolution m . Without loss of generality, we can assume that $f(x) \in V_0$ where V_m is the linear spanned by the scaling functions $\varphi_{m,n}$. Hence, we can compute $f^m \in V_m$ the discrete approximation of $f(x)$ at any resolution m [3] by

$$\begin{aligned} f^m &= A_m f^0 = \langle f(u), \varphi_{m,n}(u) \rangle \\ &= \sum_{k=-\infty}^{\infty} \bar{h}(2n - k) f^{m-1}(k) \end{aligned} \tag{3.3}$$

where φ is the scaling function generated by the dilation equation

$$\varphi_{m+1,n}(x) = \sum_{k=-\infty}^{\infty} \langle \varphi_{m+1,k}(u), \varphi_{m,k}(u) \rangle \varphi_{m,k}(u) \quad (3.4)$$

and h is the mirror filter (i.e. $\bar{h}(n) = h(-n)$) of the finite impulse response(FIR) filter $h(n)$ defined by

$$h(n) = \sqrt{2} \int_{-\infty}^{+\infty} \varphi(x) \varphi(2x - n) dx \quad (3.5)$$

By taking the inner product of f and $\varphi_{m+1,n}(x)$ in eqn. 3.4, and rearranging the terms, one can show that

$$f^{m+1}(n) = \langle f, \varphi_{m+1,n} \rangle = \sum_{k=-\infty}^{\infty} \bar{h}(2n - k) f^m(k) \quad (3.6)$$

The above in effect means that

$$f^{m+1}(n) = \bar{h}(2n) * f^m(2n)$$

If a coarse approximation $f^m \in V_m$ of $f(x, y)$ is obtained, it can be used as an initial estimate for the iterative algorithm to obtain a new finer approximation $f^{m-1} \in V_{m-1}$ of $f(x, y)$. This procedure is being repeated until $m = 0$, where the image is reconstructed at the original resolution. In the experiments under taken, normally 2 - 3 levels of decomposition were under taken. It is to be understood here that the support constraints are just as valid for the decomposed subspaces as was for the original space of full resolution($m = 0$). This in effect introduces a constraint of computing the subimage support from the subimage autocorrelation since the subspace image dimensions are different from half the original image dimensions. Therefore there was a limitation in terms of how lower(coarser) one can go to get correct solutions at the coarse levels. The alternative which was chosen was that the support at child subspace is taken approximately half the mother subspace. Though this results in some truncation of the reconstruction at the subspace level, yet to some extent an adaptive mask takes care of this.

CENTRAL LIBRARY
I. I. T., KANPUR
Ms No. A 128769

In order to reconstruct f^m , we need to use the Fourier transform magnitude at the m^{th} resolution. Since a precise measurement of those are not available at all the required resolutions, i.e., $|F^m(u, v)|; 0 < m < M$, an estimate of these measurements is obtained by taking the Fourier transform for both sides of eqn., 3.6 as follows:

$$F^{m+1}(\omega) = F^m\left(\frac{\omega}{2}\right)H\left(\frac{\omega}{2}\right) \quad (3.7)$$

Hence, the Fourier transform magnitude $|F^{(u,v)}|$ at all resolutions $m > 0$ was obtained from the Fourier transform magnitude of the image at the original resolution $m = 0$.

The approximations $f^m \in V_m$ were then obtained by performing several cycles of the basic Fienup algorithm at this resolution. The procedure was typically started by considering an array of 16×16 random numbers (since resolution level $m = 0, 1, 2$ and 3 were considered in most of the cases) as the initial guess as input to the algorithm. The autocorrelation was computed from the Fourier modulus at the original resolution and thresholded at 0.005 of the maximum value for compactness, else noise if any would have influenced the support region resulting in grossly wrong reconstructions and stagnation. An ad hoc value of 0.005 was found to be giving a satisfactory support length with the constraints of the Fourier resolution. Once the estimate of the image is obtained at the coarser resolution $f^m; m > 0$, the resulting image is expanded by a factor of two by interpolating rows and columns with zeros and preserving the dimensions of the next fine image subspace. The magnified version f_0^{m-1} becomes the initial input for the next higher resolution. Starting with this new initial estimate and the Fourier magnitude at this resolution $|F^{m-1}(u, v)|$, the same basic steps are performed at this resolution level $m - 1$. This *coarse to fine* process is repeated until the image is reconstructed at the original resolution $m = 0$.

In terms of computational efficiency, it is clear that if the number of pixels in the original resolution image was $N \times N$, then the approximate subspaces at each coarser resolution levels ($A_m f$ if original image was f) will have $2^{-m}N \times 2^{-m}N$ pixels. Since the iterative transform algorithms are computationally intensive, it is a considerable saving if one can work in the subspaces.

The normalised root mean square reconstruction error (NRMS) was hence calculated akin to the procedure as explained earlier (section 3.4.1) for all the wavelet classes.

3.6 Ambiguity Correction

As has been brought out in earlier sections (see 3.3), the reversal and translation are two ambiguities which are inherent in the phase reconstructed images when the only known input to start with is the Fourier modulus of the original image. This is due to the fact that the Fourier modulus of an array is equal to the Fourier modulus of the time shifted version as well as origin flipped (reversed) version array. Since phase retrieval from the wavelet decomposition method employs multiresolution technique, an attempt was made to correct the ambiguities before the phase retrieval actually starts at the full resolution on the finest grid. Hence at the coarsest level the reconstruction was visually seen and the ambiguities corrected in the following manner:

1. Reflection ambiguity - Two signals $x(m, n)$ and $y(m, n)$ will be said to be in reflection ambiguity if they are related by $y(m, n) = x(-m, -n)$. The Fourier modulus of both signals $x(-m, -n)$ and $y(m, n)$ are same but they are the phase

reversed version of each other which can be easily found out by the basic equation

$$\mathcal{F}[y(m, n)] = \sum_{m, n=-\infty}^{+\infty} y(m, n) e^{-j(\omega_1 m + \omega_2 n)} \quad (3.8)$$

Therefore the reconstruction was visually seen at the coarsest level and and reversal ambiguity if present was removed by reversing the phase of the subsignal obtained at that point. The iterations were thereafter allowed to proceed further with the phase reversed signal. It is notable that the algorithm preserves the phase of the signal in whatever is reconstructed the first time without further reversing or translating it.

2 Translation ambiguity - This is manifested between two signals in the form $y(m, n) = x(m + k, n + l)$. Again we note that the two signals have the same Fourier modulus. The phase of the two differ in a sense that translation in spatial domain is reflected as a modulation term $e^{-j\omega t}$ (t is the amount of translation) in the Fourier domain. Hence translation ambiguity whenever present was corrected at the coarser levels only.

3.7 Fourier coefficient truncation

The Fourier transforms of general images have been observed to have most of their energy concentrated in a small region in the frequency domain near the origin and along both the dimensions of the frequencies. The reason for this can be that typically images have maximum region where the intensities change slowly. On the other hand sharp discontinuities like edges contribute to high as well as low frequency components. Since most of the signal energy is concentrated in a small frequency region, it should be possible for an image to be reconstructed without significant loss of quality from a fraction of the transform coefficients. Therefore to illustrate

the robustness of the reconstruction by any phase retrieval method, the Fourier coefficient truncation was done to 50% and to 12% of the Fourier modulus values of the retrieved values. Rest all the transform coefficients were set to zero. It was hence shown that the reconstruction can be even attempted with fewer transform coefficients with a marginal trade off with quality and intelligibility.

Chapter 4

Reconstruction experiments and results

4.1 Fienup Reconstructions

Test images taken up for phase retrieval by Fienup algorithm in conjunction with Hybrid Input-Output algorithm were two 128×128 pixel images

- Planet Saturn
- Figure 10

The detailed program while is appended with this text, some salient aspects of the algorithm are

- The algorithm was iterated for 11 cycles with each cycle comprising of 50 iterations of Hybrid Input-Output algorithm and subsequent 10 iterations of

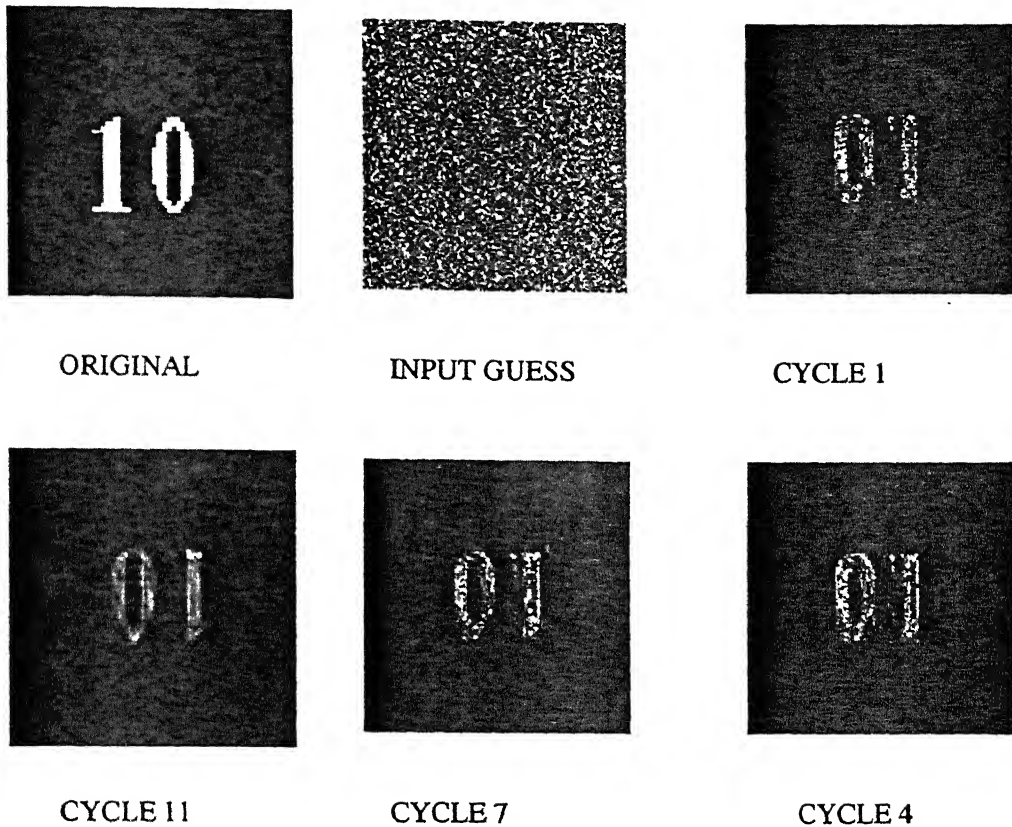


Figure 4.1: Phase retrieval by Fienup algorithm. Clockwise two images (1) original *Figure 10*. (2) initial input guess, (3) to (6) are reconstructions at increasing iterations.

4.2 Multiresolution wavelet based reconstructions

Test images taken up for multiresolution decomposition and phase retrieval were

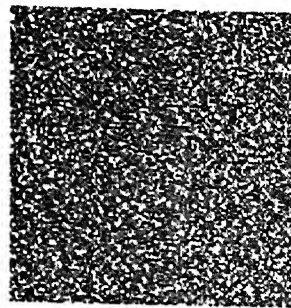
Planet Saturn

Figure 10

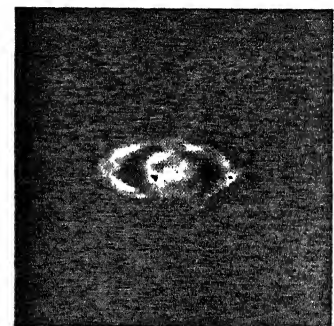
Claire



(a) ORIGINAL



(b) INITIAL GUESS



(c) RECONSTRUCTION

Figure 4.2: Phase retrieval by Fienup algorithm.(a) original *Saturn* (b) initial guess and (c) Final reconstructed image after 11 cycles

Also since the decomposition to coarser resolution levels is wavelet based, following wavelets were chosen

- Haar or Daubachies-2 length(db1)
- Daubachies 10 and 18 length (db5 and db9).
- B-Spline Biorthogonal wavelets; BiorNd.Nr as Bior4.4(full length 10) and Bior6.8(full length 18).

4.2.1 Characteristics of the wavelets used

Orthogonal and compactly supported wavelets Daubachies, Symlets and Coiflets form part of these. General properties of these class of wavelets are:

- ϕ and ψ exists and the analysis is orthogonal.
- ϕ and ψ are compactly supported.

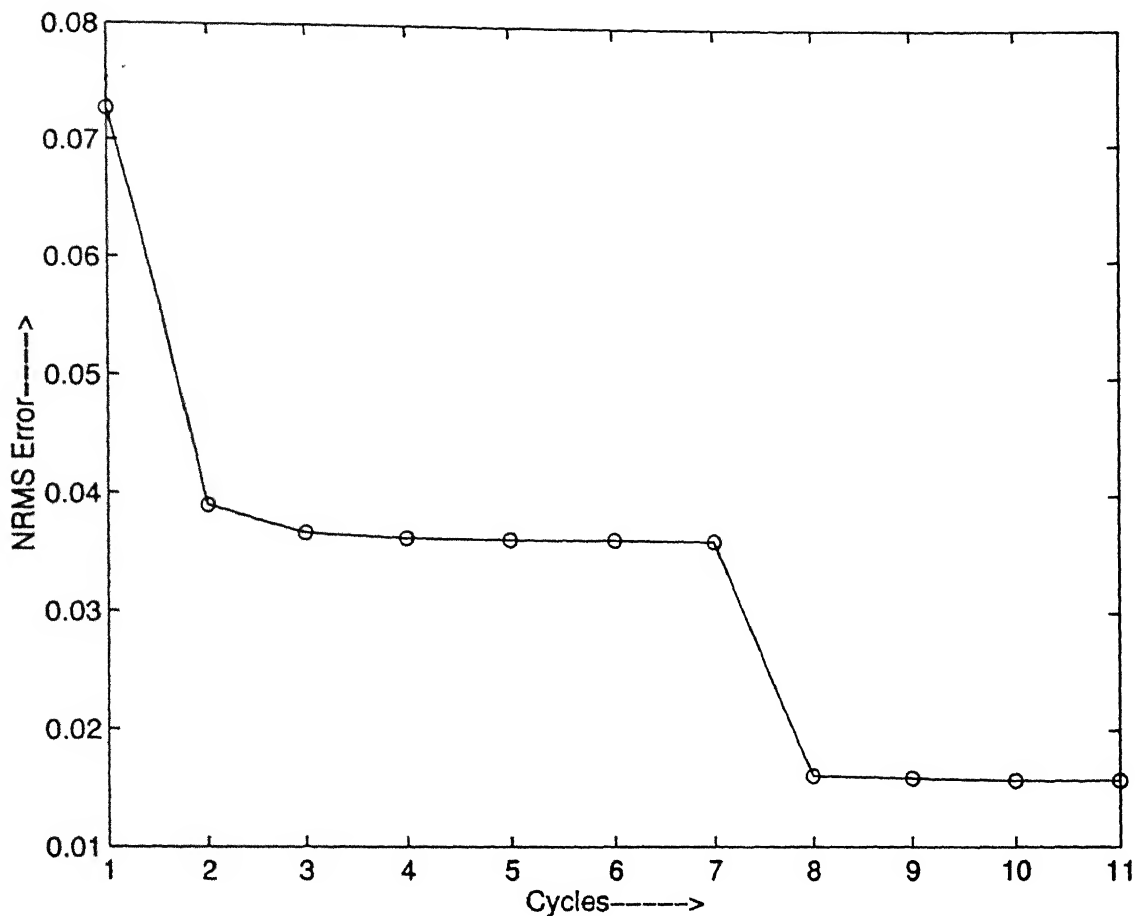


Figure 4.3: Reconstruction error for *Saturn* using Fienup algorithm for 11 cycles

- ψ has a given number of vanishing moments.
- Main nice properties of these wavelets are compact support and vanishing moments while difficulty is of poor regularity.
- Daubechies wavelets are characterised by their asymmetry.

Biorthogonal and compactly supported wavelets B-Spline Biorthogonal wavelets form part of this class. General properties of this class are:

- ϕ function exists and the analysis is Biorthogonal.

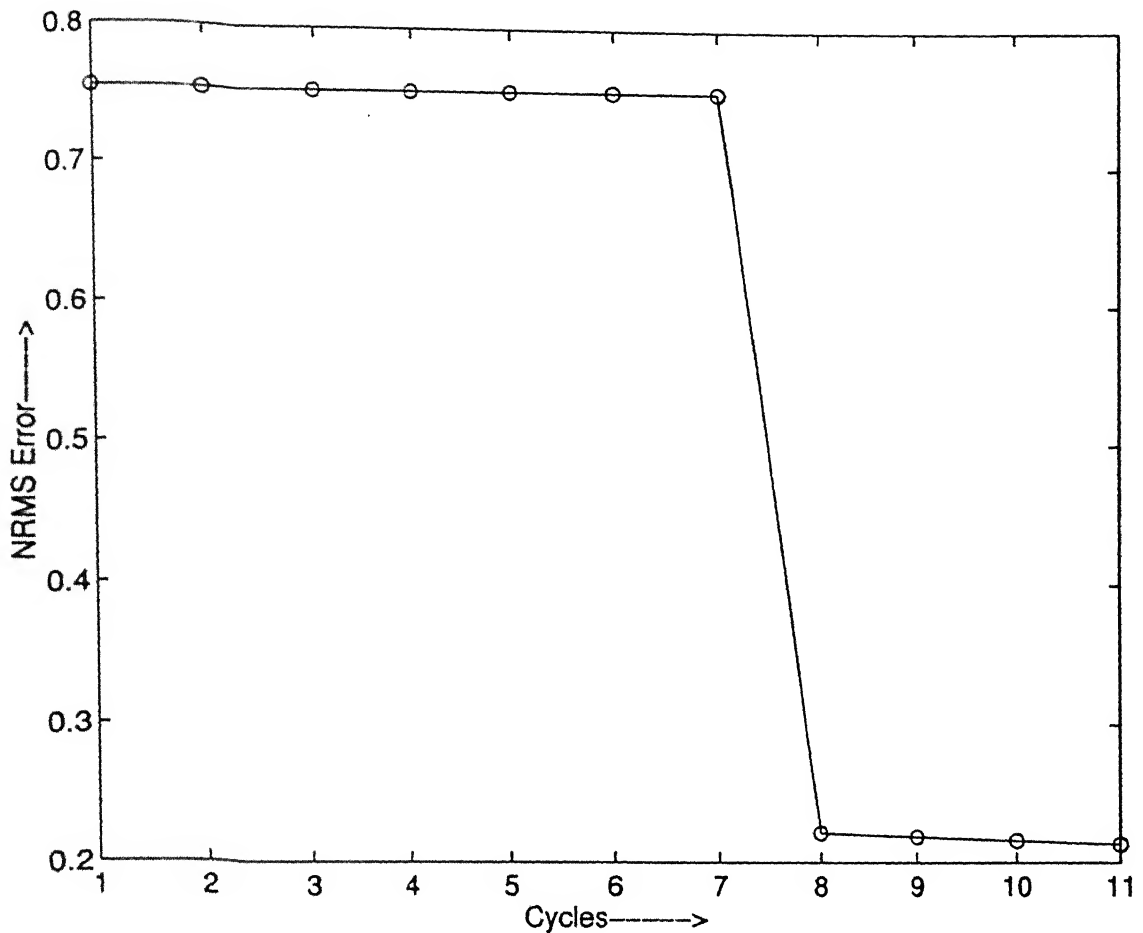


Figure 4.4: Reconstruction error for *Figure 10* using Fienup algorithm for 11 cycles

- ϕ and ψ both for decomposition and reconstruction are compactly supported.
- ϕ and ψ for decomposition have vanishing moments.
- ϕ and ψ for reconstruction have known regularity.
- Symmetry with FIR filters.
- Desirable properties for decomposition and reconstruction are splitted.
- Main difficulty is that the orthogonality is lost.

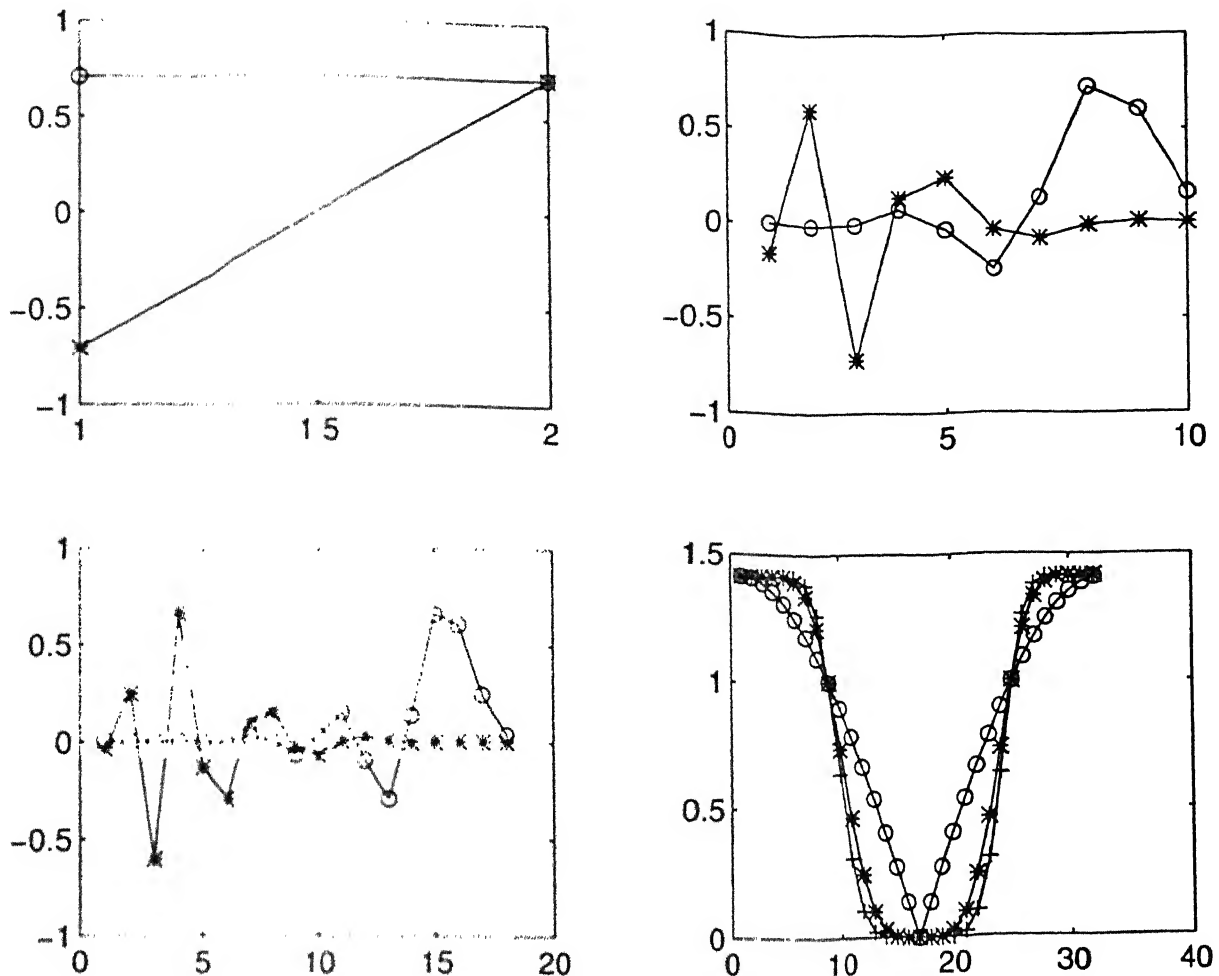


Figure 4.5: Filter coefficients and frequency responses of selected Daubechies wavelets. Clockwise from top left (a) db1 ; High(*) and low pass(○) decomposition wavelets (b) db5 (c) Frequency response of the wavelets; ○ shows db1, * shows db5 and + shows db9 low pass decomposition wavelet frequency response. (d) db9.

4.2.2 Algorithm

Some salient aspects of the algorithm are

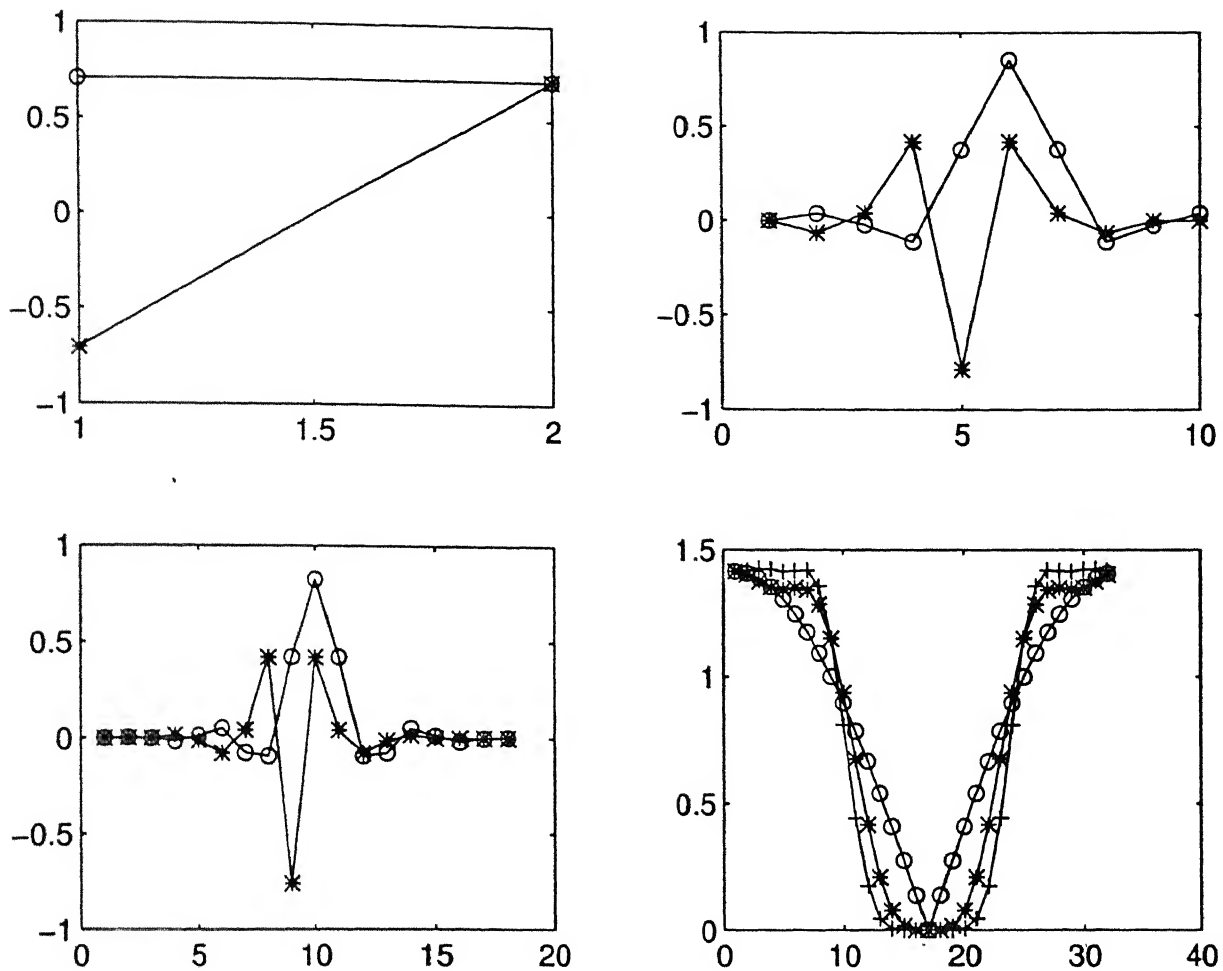


Figure 4.6: Filter coefficients and frequency responses of selected B-Spline Biorthogonal wavelets. Clockwise from top left (a) Bior1.1 ; High(*) and low pass(○) decomposition wavelets. (b) bior4.4 (c) Frequency response of the wavelets, ○ shows bior1.1, * shows bior4.4 and + shows bior6.8 low pass decomposition wavelet frequency response.(d) bior6.8.

- Three levels of decomposition were carried out i.e., $m=0, \dots, 3$ on all the three classes of images.

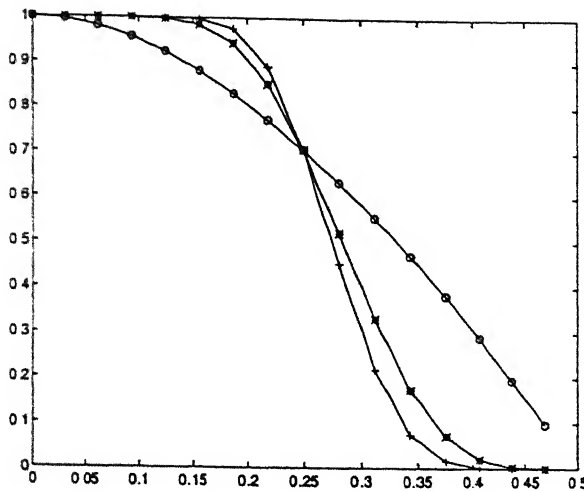


Figure 4.7: Comparative Fourier moduli of db1 (indicated on plot by \circ), db5(\star) and db9(+). All decomposition low pass characteristics.

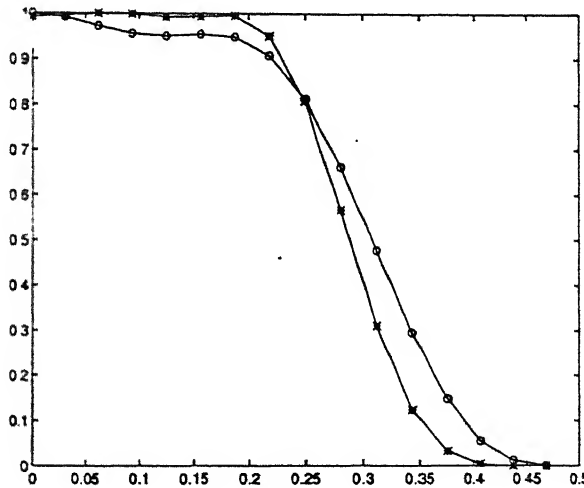


Figure 4.8: Comparative Fourier moduli of bior4.4 (indicated on plot by \circ) and bior6.8(\star). All decomposition low pass characteristics.

- The Fourier moduli at all the three levels of resolution were computed from the initial available Fourier modulus at zero(full) resolution.

Wavelet	Mean error wavelet	Fienup error	Reduction in mean error	Reduction in computations
Db1	0.0295	0.0324	9%	13%
Db5	0.0277	0.0324	15%	55%
Db9	0.0280	0.0324	14%	> 60%
Bior44	0.0296	0.0324	9%	13%
Bior68	0.0266	0.0324	18%	> 60%

Table 4.1: Reconstruction error comparisons <wavelet Vs Fienup> on image *Saturn*

- The algorithm was started by taking a 16×16 array of random numbers for the images *Saturn* and *Figure 10*. For the *Claire* image the iterations were started by taking an input guess of 64×64 array of random numbers. The iterations were kept at 30 in all for the coarser resolutions (excluding full resolution for which 60 iterations for 11 cycles were taken).
- Mask sizes were varied in a similar fashion as for the Fienup method i.e., the initial mask was computed from the autocorrelation function at the full resolution. The support at subsequent resolutions are only the demagnifications appropriate to the resolution level. Although the decomposed levels should have support somewhat greater than half the support of the previous finer subspace, yet as an initial estimate, a tighter support constraint was taken which was subsequently loosened as the iterations progressed.

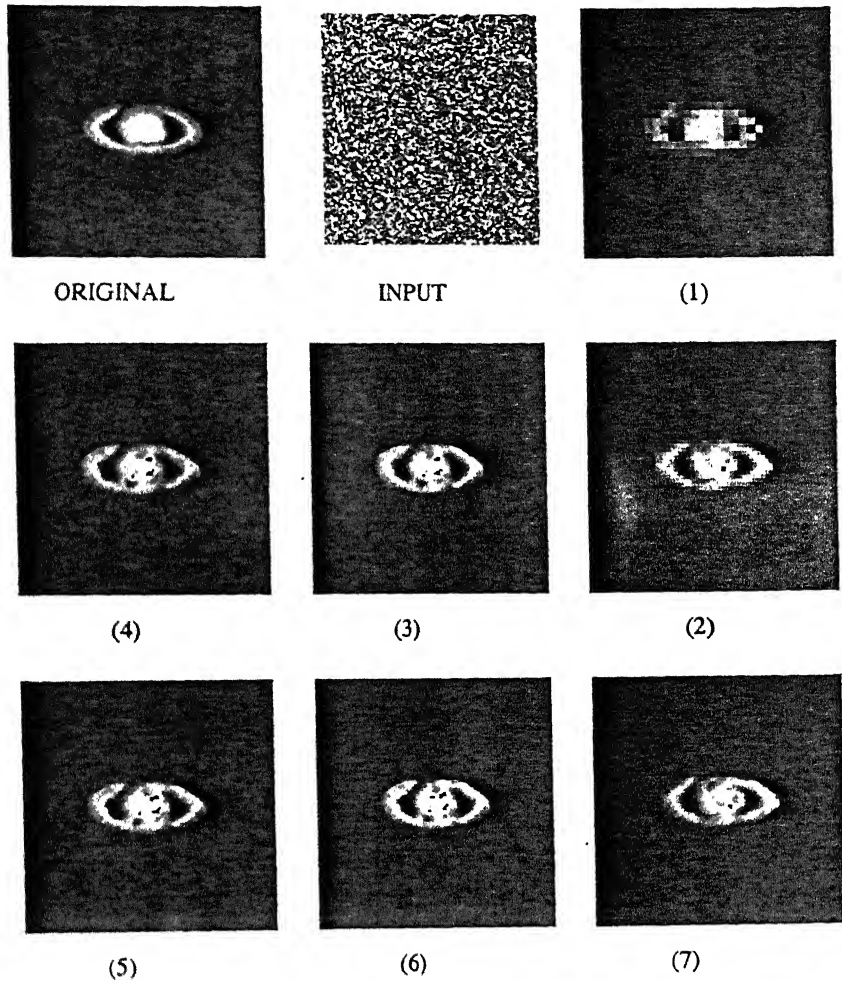
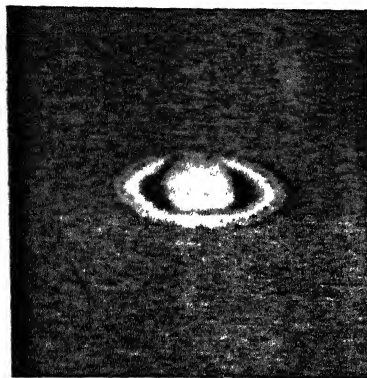


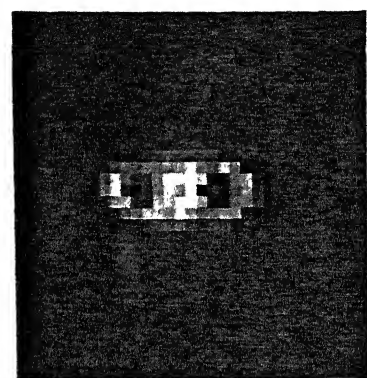
Figure 4.9: Phase retrieval by Wavelet algorithm using db5 wavelet. Clockwise from left top (a) original *Saturn* (b) initial guess and (1) Final reconstructed image at resolution 32×32 (2) reconstruction at level 64×64 resolution (3) to (7) reconstructions at increasing level of iterations for full resolution

4.3 Ambiguity correction results

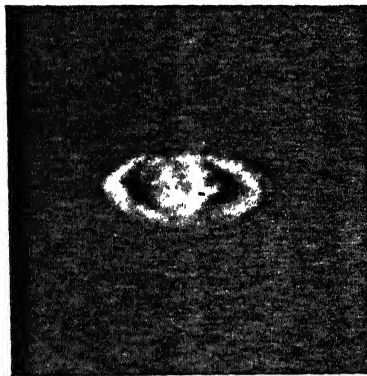
As has been brought out in previous chapter, the reversal and translation are two ambiguities which are inherent in the phase reconstructed images when the only known input to start with is the Fourier modulus of the original image. The same



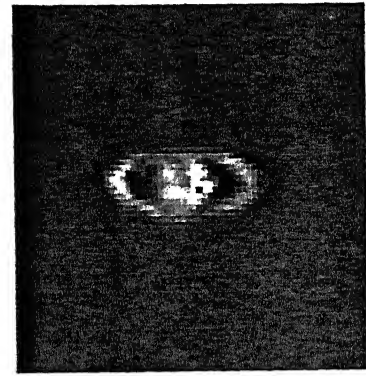
(a) ORIGINAL



(b)



(d)



(c)

Figure 4.10: Phase retrieval by Wavelet algorithm using db1 wavelet. Clockwise from left top (a) original *Saturn* (b) Final reconstructed image at resolution 32×32 (c) reconstruction at level 64×64 resolution (d) reconstruction after 11 cycles at full resolution

had been noticed in almost all the reconstructions whether partially or in full. In addition the translation ambiguity was found to be more prevalent amongst the two. These ambiguities were corrected in the manner as described in chapter 3. The results are illustrated in fig. 4.16.

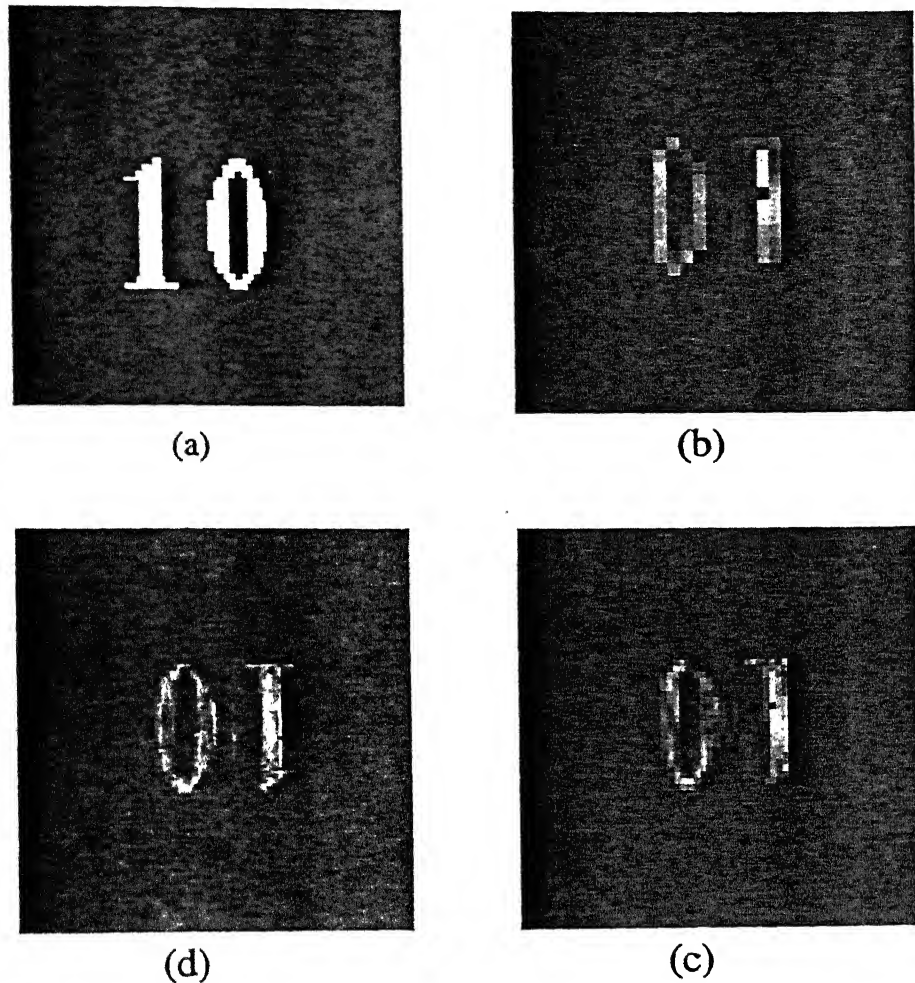
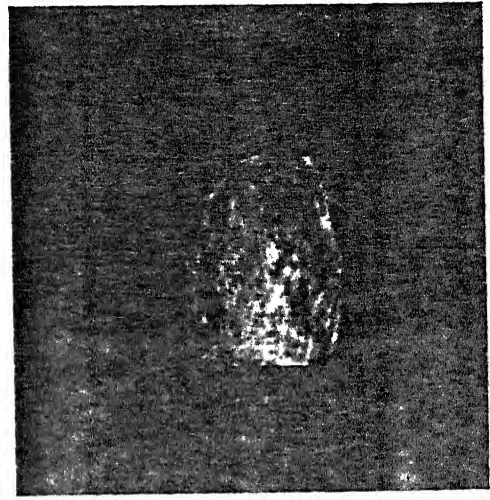
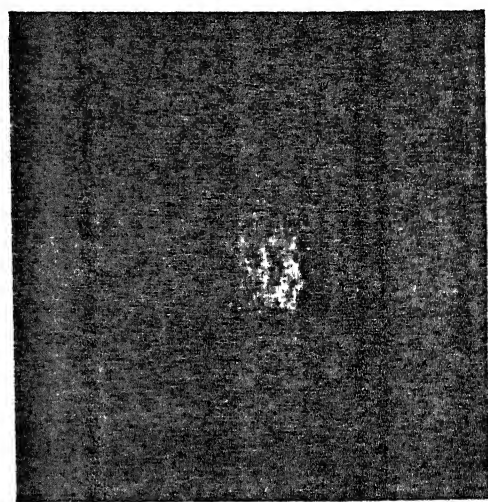
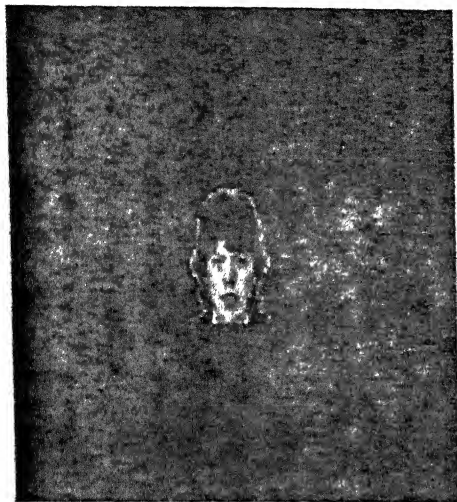


Figure 4.11: Phase retrieval by Wavelet algorithm using B-Spline Biorthogonal wavelet Bior4.4. Clockwise from left top (a) original *Figure 10* (b) Final reconstructed image at resolution 32×32 (c) reconstruction at level 64×64 resolution (d) reconstruction after 11 cycles at full resolution

4.4 Fourier coefficient truncation results

Since most of the signal energy is concentrated in a small frequency region, efficiency of iterative transform and wavelet based reconstructions can be qualitatively measured by truncation of their Fourier coefficients(i.e.,limiting the images to certain



(a)

(b)

Figure 4.12: Phase retrieval by Wavelet algorithm using db1 wavelet.(a) original *Claire* (b) Final reconstructed image at resolution 256×256 after 11 cycles at full resolution. Note that inspite of increasing the Fourier resolution, only outlines of the subject could be retrieved indicating the limitations of multiresolution phase retrieval for detailed image reconstruction with only Fourier modulus.

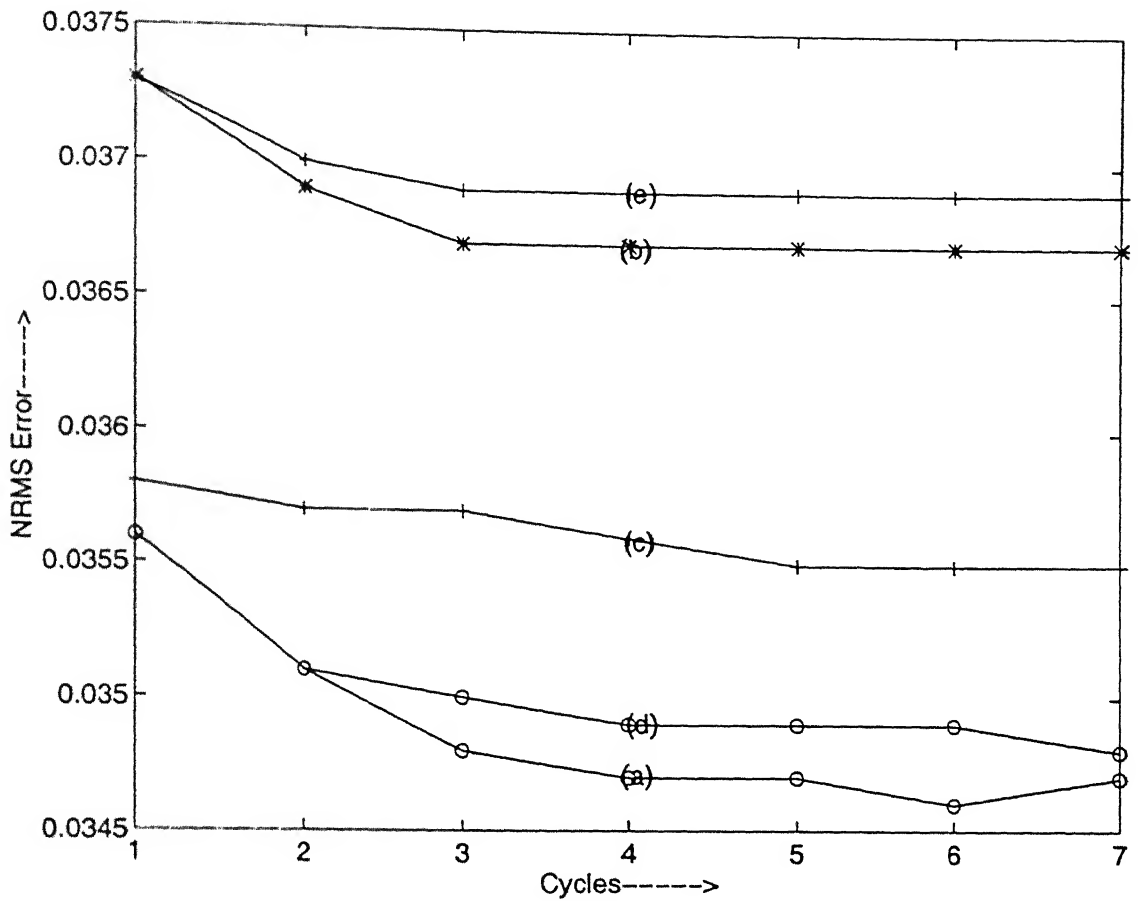


Figure 4.13: Reconstruction errors for *Saturn* using wavelet based approach for first seven cycles of iterations.(a) Using Bior6.8 wavelet (b) db1 (c) db5 (d) db9 and finally (e) Bior4.4. Convergence pattern remains same upto 11 cycles.

frequency regions only). To this effect the test images were taken and their Fourier coefficients were retained for upto 50% and 12%. The reconstruction error was although increased yet the image quality was preserved to a large extent of visual satisfaction. Quality and intelligibility were preserved without significant loss with a small fraction of the transform coefficients. Results of such comparisons are listed under table 4.1 for the *Saturn* image reconstruction with db1 wavelet and see figure

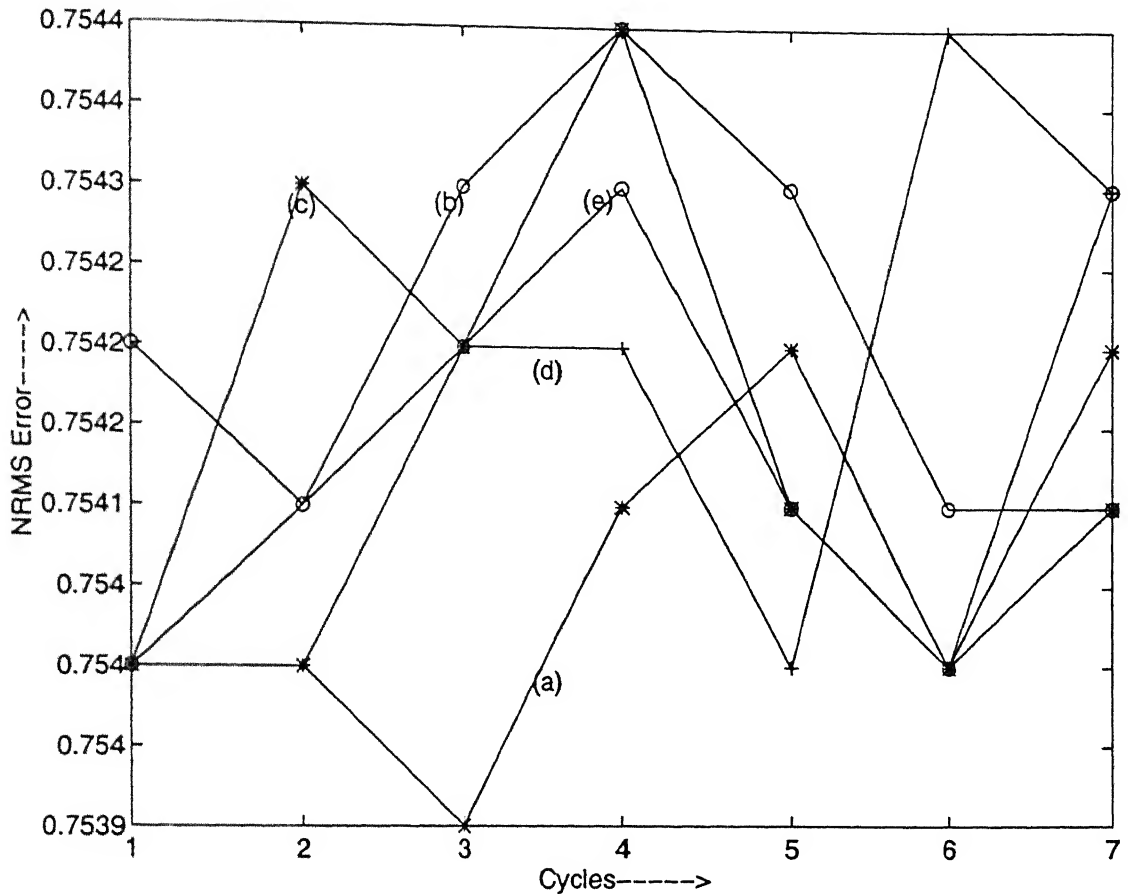


Figure 4.14: Reconstruction errors for *Figure 10* using wavelet based approach for first seven cycles of iterations. (a) Using Bior6.8 wavelet (b) db1 (c) db5 (d) db9 and finally (e) Bior4.4. Convergence pattern remains uncertain until 7 cycles wherein the mask was increased. Note that the input to the full resolution algorithm by db1 wavelet is lesser than all others.

4.17 for the reconstructions as regards *Saturn* and *figure 10*. Error results in case of *Figure 10* are similar in nature as of *Saturn*. Quality of reconstruction for all the wavelets in respect to Fourier reconstruction is satisfactory and the difference is not discernible by naked eyes due to artifacts of the viewing programs available and hence a representative figure only is being shown(*figure 4.17*).

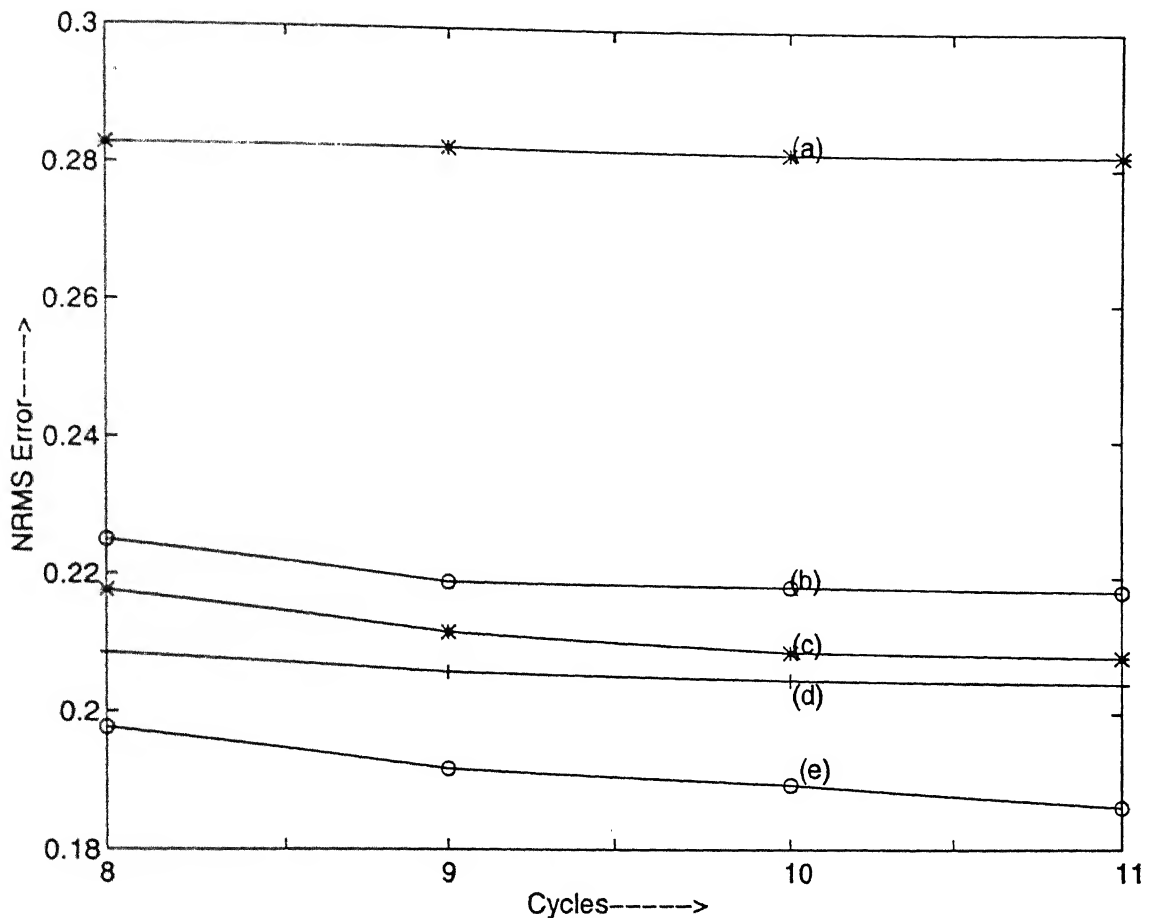


Figure 4.15: Reconstruction errors for *Figure 10* using wavelet based approach for 8 – 11 cycles of iterations.(a) Using Bior6.8 wavelet (b) db1 (c) db5 (d) db9 and finally (e) Bior4.4.

4.5 Discussions

1. The iterative transform method of phase reconstruction is a robust method and will generally retrieve the phase from a wide variety of 2-D Fourier moduli. While most images can be reconstructed satisfactorily requiring only a few cycles of iterations, other more difficult objects can require many cycles without giving satisfactory convergence and reconstruction. Confidence that

Wavelet	Mean error wavelet	Fienup error	Reduction in computations
Db1	0.5600	0.5590	<i>nil</i>
Db5	0.5569	0.5590	67%
Db9	0.5548	0.5590	67%

Table 4.2: Reconstruction error comparisons < wavelet Vs Fienup > on *Figure 10*

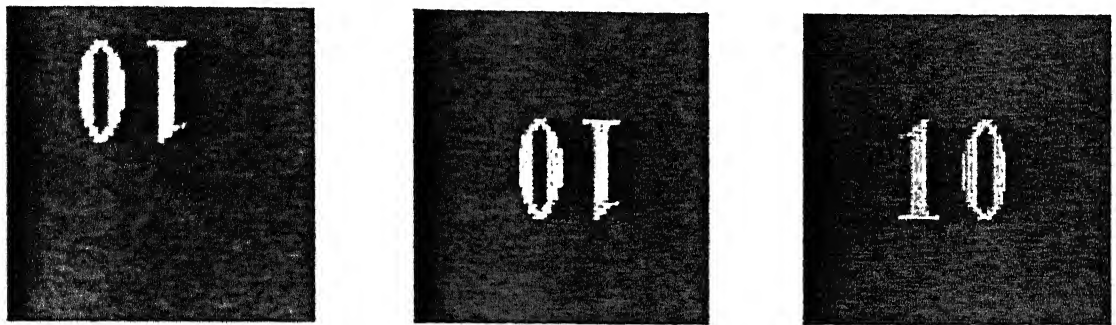


Figure 4.16: Ambiguity Corrections (a) Phase retrieved image obtained by using db5 wavelet. Note the translation and reversal ambiguities. (b) Translation ambiguity corrected image (c) Reversal ambiguity correction superimposed to get the final phase retrieved image.

the solution is the one and only true solution, can be increased by performing two or more trials of the algorithm, each time using different random numbers for the initial input.

2. The Fienup algorithm has a limitation of not being able to fill up the details in an image during reconstruction. This seems to be due to the lack of adequate reconstruction in the high frequency regions resulting in blurring of edges when there is complete lack of phase data. Consequently the Fienup algorithm does

Table 4.3: Reconstruction with truncated Fourier Coefficients

Wavelet	Percentage of retained coeffs	Now error (previous error)	Error Incr/Dcr	Reconstruction
ltd	50%	0.0407(0.0295)	27.5%	Satisfactory
-do-	12%	0.0831(0.0295)	64.5%	-do-
Db5	50%	0.0149(0.0277)	-85.9%	-do-
-do-	12%	0.0568(0.0277)	51.2%	-do-
Db9	50%	0.0498(0.0280)	43.7%	-do-
-do	12%	0.0890(0.0280)	68.5%	-do-
Bior44	50%	0.0471(0.0296)	37.1%	-do-
-do-	12%	0.0852(0.0296)	65.2%	-do-
Bior68	50%	0.0411(0.0266)	35.3%	-do-
-do-	12%	0.0863(0.0266)	69.17%	-do-

not seem to be suitable for detailed images where intelligibility measure is very exact and more biased towards human visual perception. Human facial features are a case in point here.

3. The wavelet decomposition algorithm decomposes the search space into orthogonal subspaces and hence is efficient for the following reasons:

- It gives an initial input closer to the true solution as compared to the Fienup algorithm and hence chances of getting less residual error and adequate reconstruction are greater.
- Avoids possible stagnation basins by reducing the low frequency error responsible for the slow convergence of the algorithm.

- Lesser computational complexity while working in the subspaces and overall reduction in computations as compared to the Fienup algorithm.

1. While the wavelet decomposition algorithm presents an advantage over the the Fienup algorithm, the choice of a particular wavelet depends on the following quality criterion:
 - (a) Orthogonality of the bases.
 - (b) Compactness of the wavelets.
 - (c) Regularity of scaling functions.
 - (d) Number of vanishing moments.
 - (e) Characteristics of the scaling function.

The above factors influence reconstruction error , convergence and quality in the following manner:

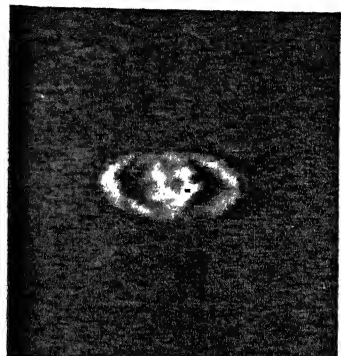
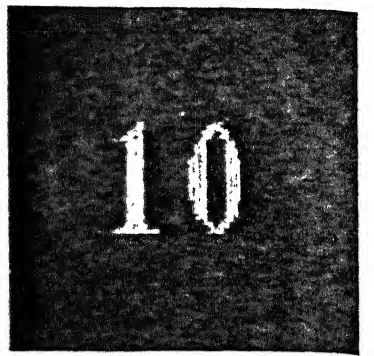
- (a) Daubachies class of wavelets are more compactly supported than the Biorthogonal spline wavelets. Hence the decompositions in the subspaces are more representative estimates than the Biorthogonal spline wavelets and therefore residual error will be less at lower resolutions for the Daubachies class wavelets.
- (b) Wavelet support(more) gives better and tighter support constraints as is obvious and hence in the same class of wavelets, a longer length wavelet will give lesser residual error. This is being borne by the results obtained wherein the reconstruction errors for lengthier filters (elements making up the support of the impulse response) are less. However although it is more likely that the initial error in case of longer length filter will be lesser as compared to shorter filter, yet the nature of iterative transform algorithm is such that the convergence pattern of the algorithm can not be clearly

predicted as the iterations progress. Many reconstruction experiments have been carried out and it can be concluded that although it is better to start with an input closer to the true solution, yet the nature of the convergence can not be predicted by initial input alone.

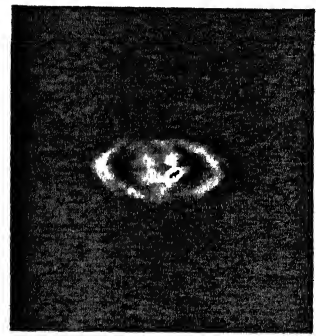
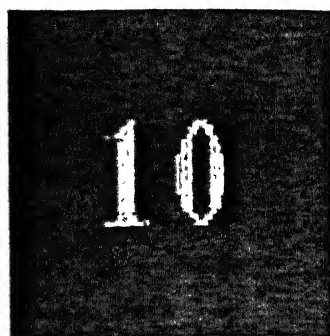
- (c) Regularity of Daubachies(α, V) class is poor when compared to Biorthogonal spline wavelets(N) and hence it is expected that it should introduce more discontinuities (artificial edges) at the coarser levels during decomposition. However since no PR is being attempted (no synthesis wavelet being used) it is understandable that the lack of higher frequencies in the reconstruction is setting aside this advantage, the Biorthogonal spline wavelets would have had if the analysis-synthesis pairs were used for reconstruction.
- (d) Linear phase filters as compared to Non linear phase filters have better decomposition properties in so far as degradation of edges is considered. However the advantage Biorthogonal spline filters would have had in this respect has been again lost for the same reasons that only modulus information of the low pass filtered image is being considered for phase retrieval.

5. Ambiguity removal from the phase reconstruction algorithm has been attempted and it has been found that once the ambiguities are removed, they will not manifest again during the reconstruction iterations. This does not seem to be incidental as has been found by many experiments. The possible cause seems to be the partially reconstructed phase characteristics. It has been experimentally established before [4] that ambiguities manifest themselves less for non symmetrically supported objects and are prominent in centrosymmetric objects because of strong symmetry around the center. Since during the course of iterations the objects are only partially reconstructed, it is likely that

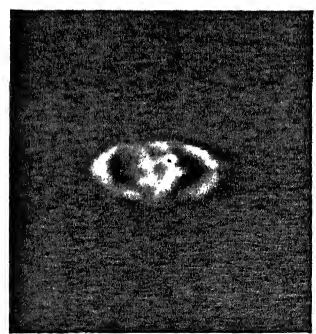
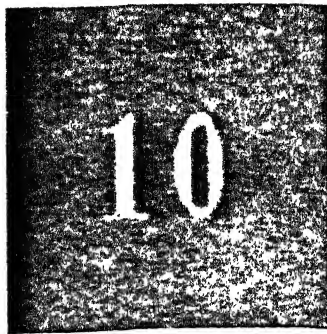
the ambiguities once corrected will not remanifest themselves.



(a)



(b)



(c)

Figure 4.17: Reconstruction of images with truncated Fourier coefficients. (a) Phase retrieved images with db1 wavelet (b) Images obtained by preserving 50% of Fourier coefficients. All others are set to 0. (c) Same with 12% of the coefficients preserved.

Chapter 5

Conclusions And Scope For Future Work

Image reconstruction from the Fourier modulus data is an important problem and as yet not fully been solved satisfactorily. Iterative transform methods, since efficient, are the most sought after algorithms in this connection. The algorithms however suffer from major disadvantages :

1. Lack of initial input guess.
2. Slow convergence and stagnation of the algorithm.
3. Intensive computational complexity.
4. Reconstruction ambiguities.

Any improvement to alter the influencing factors for image reconstruction error minimisation hence is being sought. In this the wavelet decomposition ap-

proach is being validated with the aim of suggesting an improvement in the initial input guess, the convergence rate and ambiguity removal.

The approaches are being tested with various wavelet bases and on different classes of images to reduce inconsistency in measurement errors. The effect of the wavelets used for *analysis* was studied and results summarised.

5.1 Scope for future work

It is observed that the nature of wavelets used has an effect on resultant reconstructions obtained by iterative transform algorithms. However it would be beneficial if the same is tested on a wider variety of wavelets to suggest an optimum wavelet for image analysis-synthesis for *Phase retrieval* problems.

While estimation of Fourier modulus data was taken, it is assumed that the modulus is recorded in a noise free, blur free environment. The algorithm can be suitably modified to investigate the phase retrieval from noisy Fourier modulus data.

Since an improved algorithm (ambiguities have been taken care of) is at hand, it will be of interest to use both analysis and synthesis wavelet pairs (high and low pass) in a PR fashion to integrate the high frequency details in the reconstruction at the subspace levels. This approach may improve the image reconstruction error and more so the reconstruction quality.

Bibliography

- [1] W A Rabadi and H R Myler, “Iterative image reconstruction: A wavelet approach,” *Sig. processing letters*, Vol. 5, No. 1, Jan 1998
- [2] H Stark, “*Image Recovery: Theory and Application*,” Academic press, 1987
- [3] S G Mallat, “A theory of multiresolution signal decomposition : The wavelet representation,” *IEEE Trans. PAMI.*, Vol. 11, No. 7, pp 674-693, July 1989
- [4] M H Hayes, “The reconstruction of a multidimensional sequence from the phase or magnitude of its Fourier transform,” *IEEE Trans.on ASSP*, Vol. ASSP-30, No. 2, April 1982
- [5] L S Taylor, “The phase retrieval problem,”, *IEEE Trans. Ant. and propagation*, Vol. AP-29(2), pp 386-391, 1981
- [6] J R Fienup, “Phase retrieval algorithms: A Comparison,” *Applied Optics*, Vol. 21(15), pp 2758-2769, 1982
- [7] A V Oppenheim and J S Lim, “The importance of phase in signals,” *Proc. IEEE* 69, pp 529-541, 1981
- [8] M H Hayes, J S Lim and A V Oppenheim, “Signal reconstruction from the phase or magnitude of its Fourier transform,” *IEEE Trans. Acoust., Speech,Sig. Proc.*, Vol. ASSP-28, pp 670-680, 1980

- [9] M Barlaud, “*Wavelets in image communication*,” Elsevier 1994
- [10] Y T Chan, “*Wavelet Basics*,” Kluwer Academic press, 1995
- [11] Ingrid Daubechies, “Where do wavelets come from ?-A personal point of view,”
Proc. IEEE, Vol. 84, No. 4, April 1996
- [12] A Cohen and J Kovačević “Wavelets: The Mathematical Background,” *Proc. IEEE*, Vol. 84, No. 4, April 1996

128769

128769

Date Slip

This book is to be returned on the
date last stamped.



111
EE|1999/M
671554